AD-A283 728

Miscellaneous Paper HL-94-2
July 1994

US Army Corps of Engineers
Waterways Experiment Station

Humboldt Bay Numerical Hydrodynamics and Sedimentation Study

by Robert A. Evans, Jr.

WES

Prepared for U.S. Army Engineer District, San Francisco

Miscellaneous Paper HL-94-2
July 1994

Humboldt Bay Numerical Hydrodynamics and Sedimentation Study

by Robert A. Evans, Jr.

U.S. Army Corps of Engineers
Waterways Experiment Station
3909 Halls Ferry Road
Vicksburg, MS 39180-6199

Final report

Approved for public release; distribution is unlimited

Prepared for U.S. Army Engineer District, San Francisco
San Francisco, CA 95105-1905

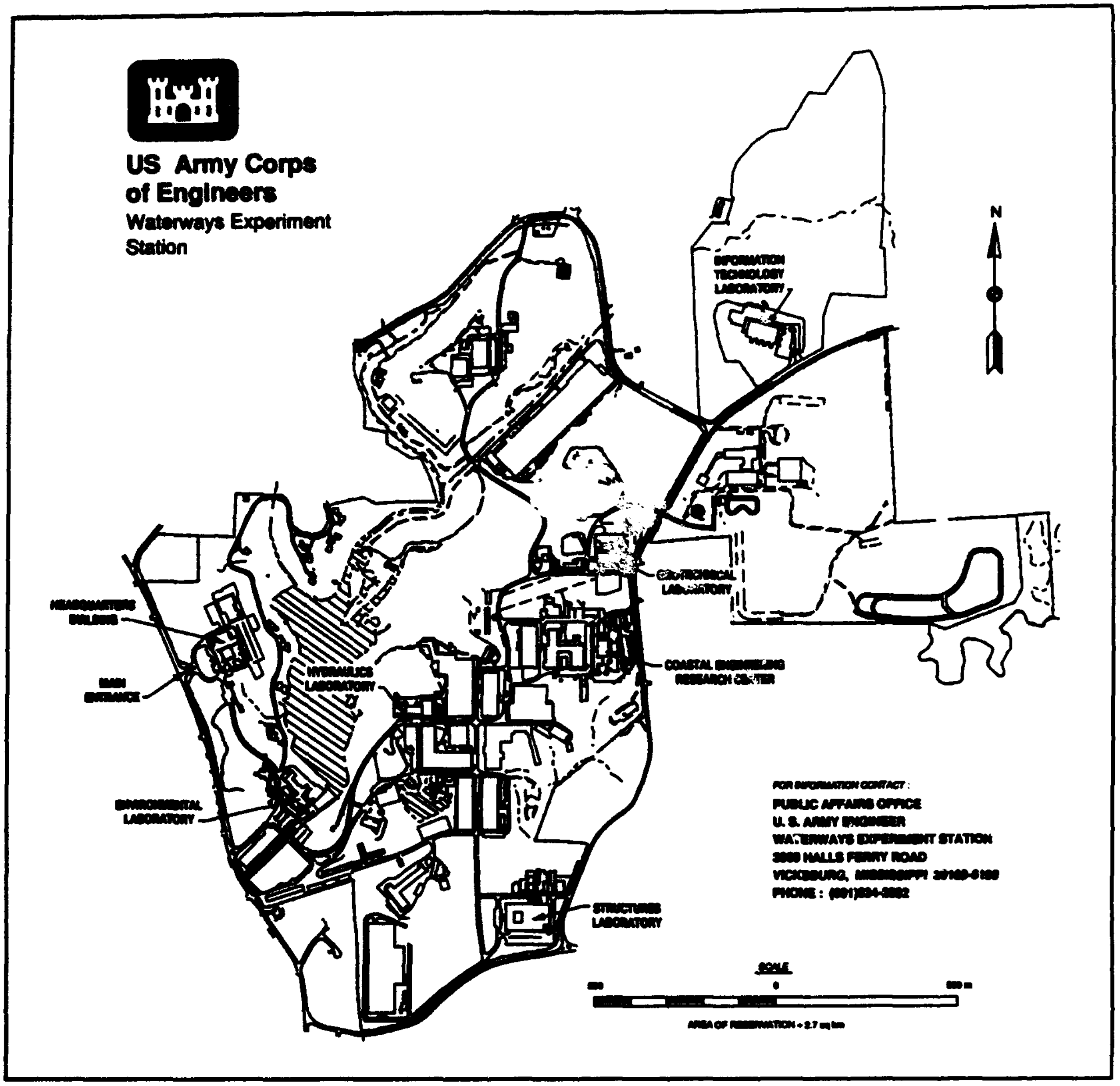

Waterways Experiment Station Cataloging-in-Publication Data

Evans, Robert A.
Humbolt Bay numerical hydrodynamics and sedimentation study / by Robert A. Evans, Jr. ; prepared for U.S. Army Engineer District, San Francisco.
67 p. : ill. ; 28 cm. -- (Miscellaneous paper ; HL-94-2)
Includes bibliographic references.
1. Ocean circulation -- California -- Humbolt Bay. 2. Sediment transport -- Mathematical models. 3. Humbolt Bay (Calif.) 4. Ocean currents -- California -- Humbolt Bay -- Mathematical models. I. United States. Army. Corps of Engineers. San Francisco District. II. U.S. Army Engineer Waterways Experiment Station. III. Hydraulics Laboratory (U.S.) IV. Title. V. Series: Miscellaneous paper (U.S. Army Engineer Waterways Experiment Station) ; HL-94-2.
TA7 W34m no.HL-94-2

Contents

Preface

The work reported herein was performed in the Hydraulics Laboratory of the U.S. Army Engineer Waterways Experiment Station (WES) as part of an investigation into the hydrodynamics and sedimentation of Humboldt Bay for the U.S. Army Engineer District, San Francisco (SPN). This report presents the results of the numerical modeling work.

The work was conducted from October 1990 to April 1993 under the direction of the following personnel: Messrs. F. A. Herrmann, Jr., Chief of the Hydraulics Laboratory; R. A. Sager, Assistant Chief of the Hydraulics Laboratory; W. H. McAnally, Chief of the Estuaries Division, Hydraulics Laboratory; D. R. Richard, Chief of the Estuarine Simulation Branch, Estuaries Division; and Project Manager R. A. Evans, Jr., Estuarine Simulation Branch.

Mr. Evans wrote this report, and Messrs. Richards and McAnally assisted in the analysis of the results.

At the time of publication of this report, Director of WES was Dr. Robert W. Whalin. Commander was COL Bruce K. Howard, EN.

Conversion Factors, Non-SI to SI Units of Measurement

Non-SI units of measurement used in this report can be converted to SI units as follows:

Multiply	By	To Obtain
feet	0.3048	meters
inches	2.54	centimeters
miles (U.S. statute)	1.609347	kilometers
pounds (force)-second per square foot	47.88026	pascal-seconds

1 Introduction

Objective

The purpose of this study was to determine the impact of proposed deepening and widening of the present ship channels on the hydrodynamics and sedimentation within Humboldt Bay. This study is part of a feasibility study which is proceeding on the basis that no General Design Memorandum (GDM) will be prepared.

Background

The Humboldt Bay system is located on the northern California coast about 260 miles[1] north of San Francisco (Figure 1). The system consists of three bays, which in a south to north order include South Bay, Humboldt (or entrance) Bay, and Arcata Bay. The only opening to the Pacific Ocean is a jettied inlet into Humboldt Bay. Deep-draft navigation channels include the entrance channel with widths from 1600 ft to 500 ft and a depth of 40 ft, Fields Landing Channel with a width of 300 ft and a depth of 26 ft, North Bay, Samoa, and Outer Eureka Channels with widths of 400 ft and depths of 35 ft, and Inner Eureka Channel with a width of 400 ft and depth of 26 ft (Figure 2).

A majority of the shoaling in the navigation channels is from material carried to the inlet by longshore transport along the Pacific coast. The primary sources of this material are the Eel River (about 10 miles south of the inlet) and the Mud and Little Rivers (about 14 and 20 miles north of the inlet, respectively) (Thompson 1971). Because of limited riverine drainage into the Humboldt Bay system, sediment of a local fluvial origin is a small portion of the total.

[1] *A table of factors for converting non-SI units of measurement to SI units is found on page v.*

Approach

Since Humboldt Bay has no significant freshwater inflow and is vertically mixed, the modeling tools used to predict both the hydrodynamics and sediment transport were vertically averaged, two-dimensional (2-D) finite element numerical models. These were able to accurately define flow circulations and sediment transport between the Pacific Ocean and the various channels in Humboldt Bay. A 2-D finite-element model is ideal for this task since the area has a highly irregular shape with significant mud flats and marsh areas (Figure 3). The Corps' TABS-MD modeling system was used to define the tidal hydrodynamics of the system and to conduct the sedimentation studies. A detailed description of TABS-MD can be found in Thomas and McAnally (1991).

The model boundaries included the region of the Pacific Ocean offshore of the inlet and all the major bays of the Humboldt Bay system. The boundary conditions were defined at the ocean with a harmonic tide. Prominent features such as secondary channels, mud flats, and marshes were also modeled. The TABS-MD hydrodynamic model, RMA-2, was used to simulate tidal flows over a 16-day period. The 16-day simulation consisted of an initial one-day spin-up period followed by a 15-day, spring-neap harmonic cycle. The one-day spin-up is necessary to remove the influence of the initial conditions of water surface elevation and velocity, which are initially set to constant values throughout the finite element mesh. The 15-day period was used for limited verification of the hydrodynamics and as input for the sedimentation model, STUDH. The study scope of work did not include collection of a synoptic data set for a more complete verification of the hydrodynamics or sediment transport. An analysis of harmonic tides and velocities in the region was used to give insight into the behavior of the flows and was the basis for the limited verification.

Four geometry conditions were modeled. The following geometries tested are as described below and are shown in Figure 4 for the entrance:

a. Base (existing) condition.

b. Plan 1 - Bar and Entrance Channel deepened to 48 ft and the channel width increased and realigned as indicated by the dashed lines in Figure 4; North Bay, Outer Eureka, and Samoa Channels deepened to 38 ft; the intersection of the entrance and North Bay widened; and, Samoa Channel Turning Basin enlarged.

c. Plan 2 - The channels deepened and widened as in Plan 1, with the entrance channel widened according to the alternative plan suggested by the ship simulation study. The additional widening is indicated by the shaded area in Figure 4.

d. Plan 3 - The channels deepened as above, but not widened.

2 Hydrodynamic Model Verification

Model Boundary Conditions and Parameters

The hydrodynamic simulations covered a period of 16 days. This included a 25-hr spin-up time and 15-day spring-neap cycle. No freshwater inflows were specified. A dynamic water level boundary condition at the ocean boundary was specified. This was synthesized from National Ocean Service (NOS) harmonic constituents, with hour 0 equal to 00:00 on 24 February 1992. Eddy viscosity values were based on cell size and Peclet number (or cell Reynolds number, $P = 1.94\ UL/\varepsilon$, U = average velocity, L = average length, ε = eddy viscosity). Flow over the marshes was simulated using the marsh porosity option in TABS-MD. Elements were assigned to specific groups or types based on size, location, and average depth. The viscosities assigned to each of these types were computed based on an average length dimension of each computation mesh element and the highest expected velocity in that type. Since all the elements of a specific type were not generally oriented in the same direction, the average value of the greatest length (the longest leg of a triangle or the longest diagonal of a quadrilateral) of each element in a specific type was used for selecting the viscosity used in the hydrodynamic model. An initial estimate of 40 was used for the Peclet number to generate viscosity values. The viscosity values were changed to adjust the model results, and therefore, the final Peclet values also were changed. Roughness (Manning's n) was based on water depth and geographic location (i.e., marshes were set rougher than river channels). The viscosity, Manning's n, and approximate Peclet number for each type are listed in Table 1. Both Manning's n and eddy viscosity were adjusted to give the best verification. Although n values of 0.010 and 0.100 seem a bit extreme, they gave the best results for this study. Many densely vegetated marshes do indeed exhibit roughness characteristics that require an n value of 0.100. However, the value of 0.10 for the channel is more numerically than physically based. To get the proper lateral distribution of velocities between deep water and a wetting and drying marsh boundary with an affordable amount of mesh resolution, it was necessary to exaggerate the effects of friction. Exaggeration of lateral friction distributions has been

Table 1
Viscosity, Manning's n, and Peclet Number

Type	ε, Viscosity lb-sec/ft^2	Manning's n	Peclet Number	Average Element Length, ft	Type of Area
1	50.00	0.010	65	850	Shallow Channels
2	50.00	0.010	80	614	Main Channels
3	170.00	0.010	40	3280	Open Ocean
4	250.00	0.100	10	1317	Low Marshes
5	170.00	0.010	40	1380	From Jetties to Ocean
6	200.00	0.100	15	1773	High Marsh & Mud Flats

used in other studies and by other researchers to improve verification in tidal wetting and drying problems.[1]

Hydrodynamic Model Verification

To verify a hydrodynamic numerical model, it is preferable to have a number of locations for comparison at which water elevation and velocity is recorded simultaneously over one or more tidal periods. Since no synoptic data were available for this study, harmonic tidal data synthesized from NOS harmonic constituents were used. The harmonic data were based on an analysis of historical tides. For this study, the NOS subordinate stations at the Humboldt Bay entrance (NOS station 787), Fields Landing (NOS station 791), and Eureka Slough Bridge (NOS station 797) were used to aid in verification of the model. Note that the various harmonic constituents and phase differences for the tides are based on simultaneous observations at the reference station at Crescent City, California (NOS station 805) and at the subordinate locations.

Figure 2 shows the Humboldt Bay system with channel centerline locations and the three tide data locations. The harmonic tide at the entrance was used at the ocean boundary for the tidal boundary condition (Figure 5). The accuracy of the reconstructed tide at the subordinate stations depends on the length of time the simultaneous observations were made and the distance away from the reference stations. Eureka Slough tidal constituents are based on a simultaneous observation period of 7 months (April-October 1978), Fields Landing on a period of 9 months (April 1978-January 1979), and Humboldt

[1] Ian King, personal communication, University of California, Davis.

Bay entrance on a period of 1 year (1979). Each was referenced to Crescent City, California (personal communication with Tom Kendrick, Coastal Estuarine and Oceanography Branch, National Ocean Service, Rockville, MD). Note that the distance from Crescent City to Humboldt Bay is approximately 70 miles. The recorded tidal elevations at subordinate stations are used in conjunction with tidal records at Crescent City to derive harmonic tidal constituents. The derived values are affected by both the geometry between the reference and observation stations and by the length of time for which tidal data was sampled. The geometry between Crescent City and Humboldt Bay entrance consists of open ocean that is both simple and deep and changes little from year to year. Therefore, tidal components derived for the Humboldt Bay entrance (based on Crescent City) should have little geometry induced error. However, the interior geometry of Humboldt Bay is more complex and significant changes could occur from year to year. This results in larger geometry induced error for the interior stations of Humboldt Bay than observed at the entrance. In addition, the simultaneous sampling periods of the interior locations are shorter than that of the entrance, leading to less accuracy in the tidal constituents. In general, the subordinate stations provide fairly good guides for predictions of water elevations, but the prediction accuracy of the interior stations will be less than that of the entrance.

The difference between the water surface elevations predicted by the RMA-2 model and that predicted by harmonic synthesis at the entrance is shown in Figure 6. The largest difference is less than 0.1 ft. Figures 7 and 8 show the model results and the harmonic synthesis at Eureka Slough Bridge and Fields Landing, respectively. These results show less agreement (maximum differences of -1.0 ft at Eureka Slough Bridge and -0.6 ft at Fields Landing) and are probably due at least in part to the inaccuracy of the harmonic constituents as discussed above. These harmonic data can only be used as a guide to verification, not as absolute data.

Tidal Spectra

In an effort to further evaluate the model verification, Fast Fourier Transforms (FFT) were performed on the tidal elevations of both the model outputs and the harmonic data for the entrance, Eureka Slough Bridge, and Fields Landing. Figures 9 through 11 show the FFT's for both the model and harmonic synthesis results at the entrance, Eureka Slough Bridge, and Fields Landing, respectively. Note that the *Y* axis is logarithmic. The plot on the top of each figure shows the spectrum for frequencies between 0 and 0.4/hr (corresponding to periods of ∞ and 2.5 hr, respectively); the bottom is an enlargement for frequencies between 0 and 0.12/hr (corresponding to periods of ∞ and 8.3 hr, respectively). Also shown are the peaks corresponding to the O1 (Principal lunar diurnal, period = 25.82 hr), the K1 (Luni-solar diurnal, period = 23.93 hr), and the M2 (Principal lunar, period = 12.42 hr) tidal constituents. These show that the model is reproducing the main constituents of the harmonic tides fairly accurately. The largest inaccuracy in the spectrum is at the 0/hr, or DC frequency. The spectrum amplitude differences cannot be

distinguished from the plots, so they are listed below. These show that the entrance has the best agreement between model and harmonic predictions, Fields Landing the second best, and Eureka Slough Bridge the worst.

	0/hr Amplitude (ft-hr)		
Tidal Station	RMA-2	Harmonic	Difference
Entrance	3422	3430	8
Fields Landing	3430	3738	308
Eureka Slough Bridge	3437	4045	608

Water Velocities of the Plan Tests

Figures 12 and 14 show the general pattern of flow at flood and ebb, respectively, for the Base condition. Figures 13 and 15 show the velocity magnitude contours for the same times. From the NOS current tables, the maximum flood and ebb velocities for Humboldt Bay entrance are 2.7 and 3.4 ft/sec, respectively. The velocities predicted by RMA-2 show good agreement with these values. Figures 16 through 27 show the flood and ebb patterns and velocity magnitudes at the same times for the three plans. In general, while the flow patterns do not change significantly, the velocities of the plans decrease. This decrease is due to the increased cross-sectional area of the plans.

Figures 28 and 29 show the average velocity magnitude over the spring-neap period versus the distance from project mile 0. The velocities were extracted for center lines through the navigation channels. The first centerline runs from the end of the jetty through the entrance Channel and then northward through North Bay Channel. The center lines for both Samoa and Eureka Channels begin at this point. The centerline for Fields Landing Channel starts at the intersection with the entrance channels and runs in a southerly direction to Fields Landing. The results show that for all plans, the average velocity tends to be less than for the Base condition. The plan with the largest change in cross-section, Plan 1, shows the largest change in velocity. Plan 3, with the smallest change in cross-section, shows the least change in velocity. Plan 2, which has the same channel dimensions as Plan 1 from approximately mile 1 to the ends of Eureka and Samoa Channels, shows only slight velocity differences from Plan 1 in the entrance channel.

Water Surface Elevations of the Plan Tests

There is concern that increasing the depth and/or width of the navigation channel could affect sensitive aquaculture locations in Arcata Bay. Figures 30

through 41 examine the change in average high and low water surface elevations for the various plans. Each figure presents the change in high water in the top plot and the change in low water in the lower plot. The upper curve in each plot represents the Base average high or low water level over a 15 day spring-neap cycle, referenced to Mean Lower Low Water (MLLW). The lower curve in each plot represents the (Base-Plan) difference. The appropriate scale for the average water level is to the left, the scale for the difference is to the right, as indicated by the arrows. Note that the scale of the difference values is five times the scale of the high and low water elevations. No plan shows an absolute high or low water difference greater than 0.04 ft.

Figure 42 shows the predicted (Base) tide at Mud River Slough (see Figure 2 for location) for a 26-hr period, with the difference of Base-Plan for each of the three plans. Note that the scale on the left is for the water surface elevation while the scale on the right is for the difference and is larger by a factor of 10. This illustrates that the maximum deviation in water surface elevation is less than 0.1 ft and that the maximum deviations occur at or near mid-tide, not high or low tide. This further supports the premise that the planned channel changes will not significantly affect the tide ranges.

3 Sediment Model Verification

Sedimentation processes were simulated using the computer model Sediment Transport in Unsteady, 2-Dimensional Flow, Horizontal Plane (STUDH). This program computes the transport, deposition, and erosion of sediments in two-dimensional open channel flows. STUDH will model both cohesive (clays) and non-cohesive (sands) sediments. Grain size, fall velocity, water surface elevation, x-velocity, y-velocity, diffusion coefficients, bed density, and roughness coefficients must be defined as inputs to STUDH. The hydrodynamic input to STUDH were computed by RMA-2. A detailed description of STUDH can be found in Thomas and McAnally (1991).

Sediment Data

As stated above, the main source of sediment in the channels is sand coming in from the Pacific Ocean through the inlet. The sediment is fairly well distributed with larger sizes predominant in the inlet and smaller sizes inland. The northern channels contain medium to fine sand and Fields Landing Channel contains fine sand.

STUDH uses the Ackers-White (1973) formula for non-cohesive transport. This formula uses the d_{35} grain size (grain size at which 35% of the sample is finer). Based on this information, the sediment sizes for the numerical sediment transport model, STUDH, were determined. The base grain size was 0.3 mm with a shape factor of 7. However, STUDH allows the grain size for transport to be adjusted by node. The grain size for transport was defined by location. The ocean area grain size was set at 0.4 mm; grain size from the entrance channel to the intersection with the North Bay and Fields Landing Channels was also set to 0.4 mm. The grain size in North Bay Channel was reduced from 0.4 to 0.05 mm (medium to very fine sand) linearly over a distance of 1000 ft from the intersection northward; beyond that range, the size was a constant 0.05 mm. The size in the Fields Landing Channel and all marsh and mud flats was set at 0.05 mm. These sizes are consistent with sediment analysis described in the literature (Gast and Skeesick 1964; Thompson 1971). All fall velocities were based on the transport sediment size with the exception

of the ocean area, which had a settling velocity of 0.0 m/sec. Since no wind-wave action was simulated in the open ocean, which would normally keep much of the sediment suspended, the fall velocity there was set to zero. The maximum fall velocity was W_0 = 0.06 m/sec, corresponding with the maximum transport size of d_0 = 0.4 mm. The relationship used to determine the fall velocities for the smaller sizes was $W(d) = Kd^2$, where W is in m/sec, d is in mm, and $K = W_0/d_0^2$. These equations are derived from the equation for the fall velocity of spheres with constant gravitational acceleration, kinematic viscosity, and specific weight of the fluid (Vanoni 1975, Equation 2.2).

The initial sediment concentration in the ocean was defined to be 0.100 kg/m^3. This value was determined by trial and error, since no actual concentrations were available. To generate an initial concentration field for the area of interest, a 15-day simulation was made with an initial concentration of 0.100 kg/m^3 at all locations. The concentration field at the end of this simulation was then used to define the initial concentration for all locations, with the exception of the ocean which was kept at 0.080 kg/m^3, for the next 15-day simulation. Only the results of the second simulation were used to predict shoaling rates.

Manning's n values were defined at each node, base on the roughness values used to compute the hydrodynamics with RMA-2. The values were adjusted to get the best sedimentation results from STUDH and ranged from a high value of 0.067 (marshes and mud flats) to a low of 0.0067 (all others areas). These values were used with Manning's equation to compute the bed shear stress.

Field Data versus Model Results

Average shoaling rates were estimated based on yearly dredging volumes. Reduced to cubic meters/day, the prototype shoaling rates for the various channels were as follows (Hubertz and Brown 1991):

Channel	Shoaling Rate cu m/day	Period
Bar & Entrance	1182	(1954-1967)
Bar & Entrance	1334	(1976-1989)
North Bay	251	
Samoa	21	
Fields Landing	105	
Eureka	21	

The top of Figure 43 shows the measured and predicted shoaling rates for the five channels. Note that the Bar and entrance channel measured rate is for the most recent period (1976-1989). The rates predicted by STUDH are the total volume over a spring-neap cycle, divided by the time (15 days) and are as follows:

Channel	Shoaling Rate cu m/day
Bar & Entrance	1437
North Bay	214
Samoa	6
Fields Landing	43
Eureka	6

The predicted results are relatively close to the measured values. Sediment models which show order-of-magnitude agreement are normally considered adequate. These results show much better than an order-of-magnitude agreement. Specifically, the channels with the largest amount of shoaling, the Bar and entrance and the North Bay, show differences between predicted and measured of only 7 and 17 percent, respectively.

Sedimentation of the Plan Tests

The bottom of Figure 43 shows the shoaling rate for Base, Plan 1, Plan 2, and Plan 3 conditions. The results, in tabular form, are as follows:

	Shoaling Rate cu m/day			
Channel	Base	Plan 1	Plan 2	Plan 3
Bar & Entrance	1437	1734	1268	1498
North Bay	214	202	137	200
Samoa	6	6	4	4
Fields Landing	43	41	29	42
Eureka	6	5	4	5

Figures 44 and 45 show the sediment concentrations at a high and low tide for the base. This shows that the concentration decreases rapidly with distance away from the inlet.

Figures 46 through 49 show the total bed change for the Base, Plan 1, Plan 2, and Plan 3 geometries, respectively. The most noticeable difference is

the variation in the 1-inch (14.96 day change) contour at the tips of the jetties in Plan 2. For the Base and Plans 1 and 3, this contour is basically a straight line perpendicular to the jetties. For Plan 2, the sediment is settling much farther toward the ocean in a V shape. Also, all geometries except Plan 2 have a 5 inch bed change contour. This indicates that the lower water velocities of Plan 2, combined with the small cross-sectional area at the entrance inhibits the flow of sediment from the ocean much more effectively than the other geometries.

4 Conclusions

As stated in the first paragraph, the purpose of this study was to determine the impact of proposed deepening and widening of the present ship channels on the hydrodynamics and sedimentation within Humboldt Bay. Three plan geometries were studied. Plan 1 had the navigation channels deepened and widened according to the District's design; Plan 2 had the channels deepened and widened according to the alternative plan suggested by the ship simulation study; Plan 3 had the channels deepened only.

The results from the hydrodynamics indicate that by deepening and/or widening the channels, the velocities will decrease due to an increase in cross-sectional area. The tide range will not be significantly changed.

The results for the sedimentation study indicate that Plan 1 will have the largest amount of shoaling increase, due both to a larger cross-section at the ocean and the increased channel area. Plan 2 seems to have a significantly lower inflow of sediment than all other geometries, including the Base.

References

Ackers, P., and White, W. R. (1973). "Sediment transport: new approach and analysis," *Journal of the Hydraulics Division, American Society of Civil Engineers*, No. HY11.

Gast, James A., and Skeesick, Delbert G. (1964). "The circulation, water quality, and sedimentation of Humboldt Bay, California," Division of Natural Resources, Department of Oceanography, Humboldt State College, Arcata, CA.

Hubertz, J. M. and Brown, W. A. (1991). "A summary of information related to sediment transport estimates at Humboldt Bay California," Coastal Engineering Research Center, 1 July 1991.

Thomas, W. A. and McAnally, W. H., Jr. (1991). "Users' manual for the generalized computer program system: open-channel flow and sedimentation, TABS-2," Instruction Report HL-85-1, U.S. Army Engineer Waterways Experiment Station, Vicksburg, MS.

Thompson, Robert W. (1971). "Sedimentology and geologic history of Humboldt Bay, Eureka, California," Final Report PRF#789-G2, Geography Program, Office of Naval Research.

Vanoni, V. A., ed. (1975) "Sedimentation engineering," Manuals and Reports on Engineering Practice—No. 54, American Society of Civil Engineers, New York.

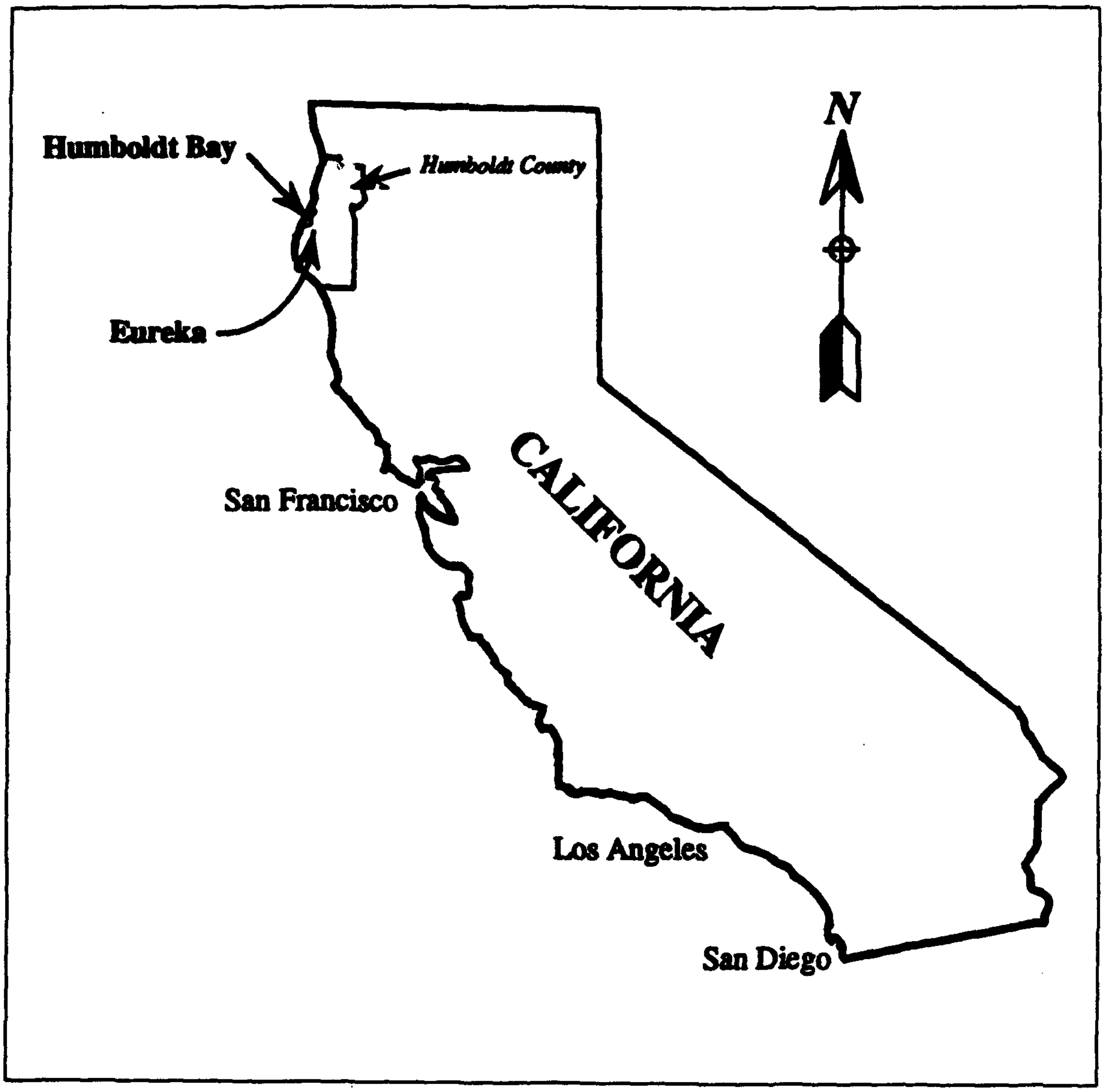

Figure 1. Location map for Humboldt Bay

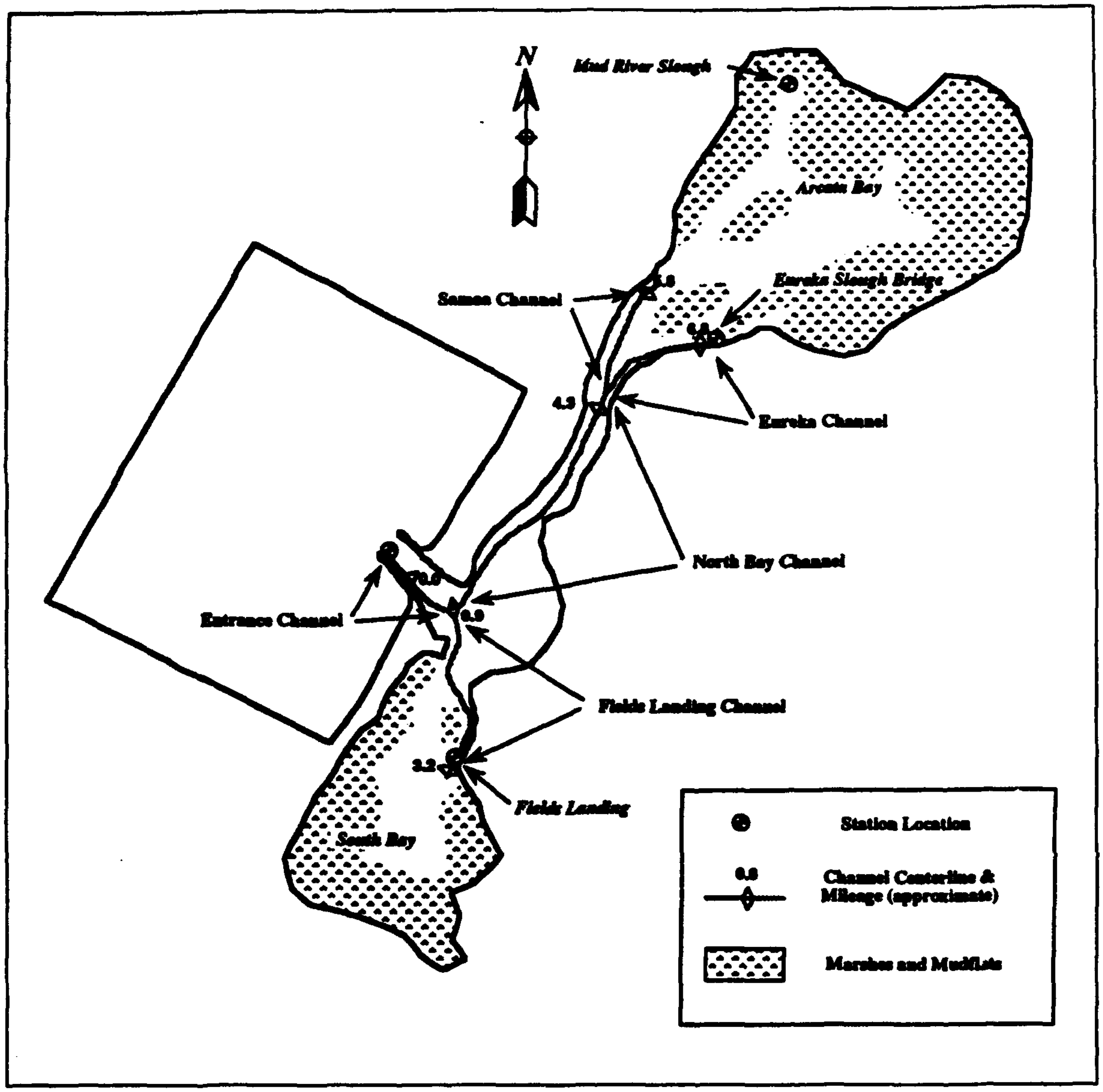

Figure 2. Humboldt Bay Channel and Station locations

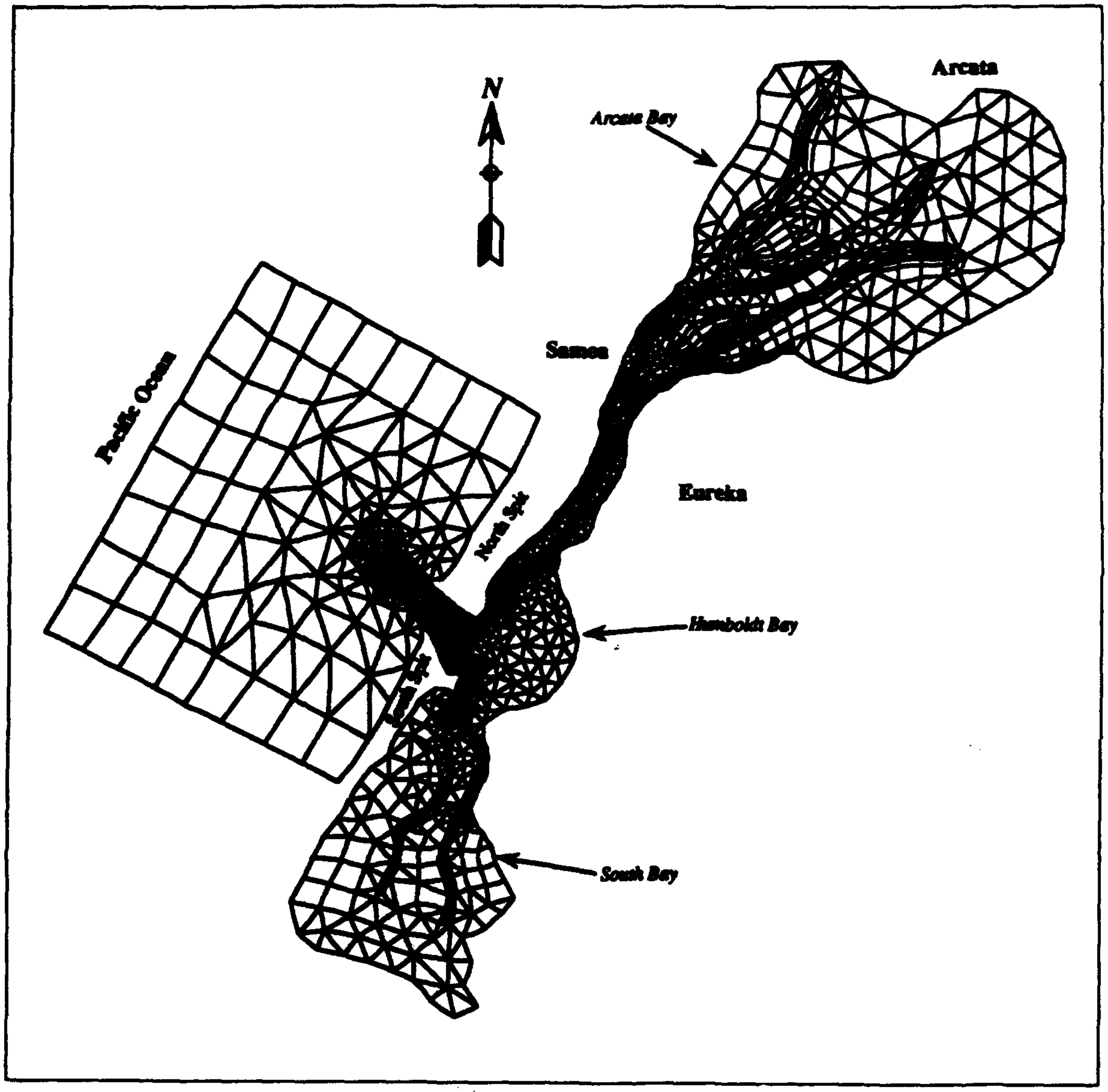

Figure 3. Humboldt Bay finite element mesh

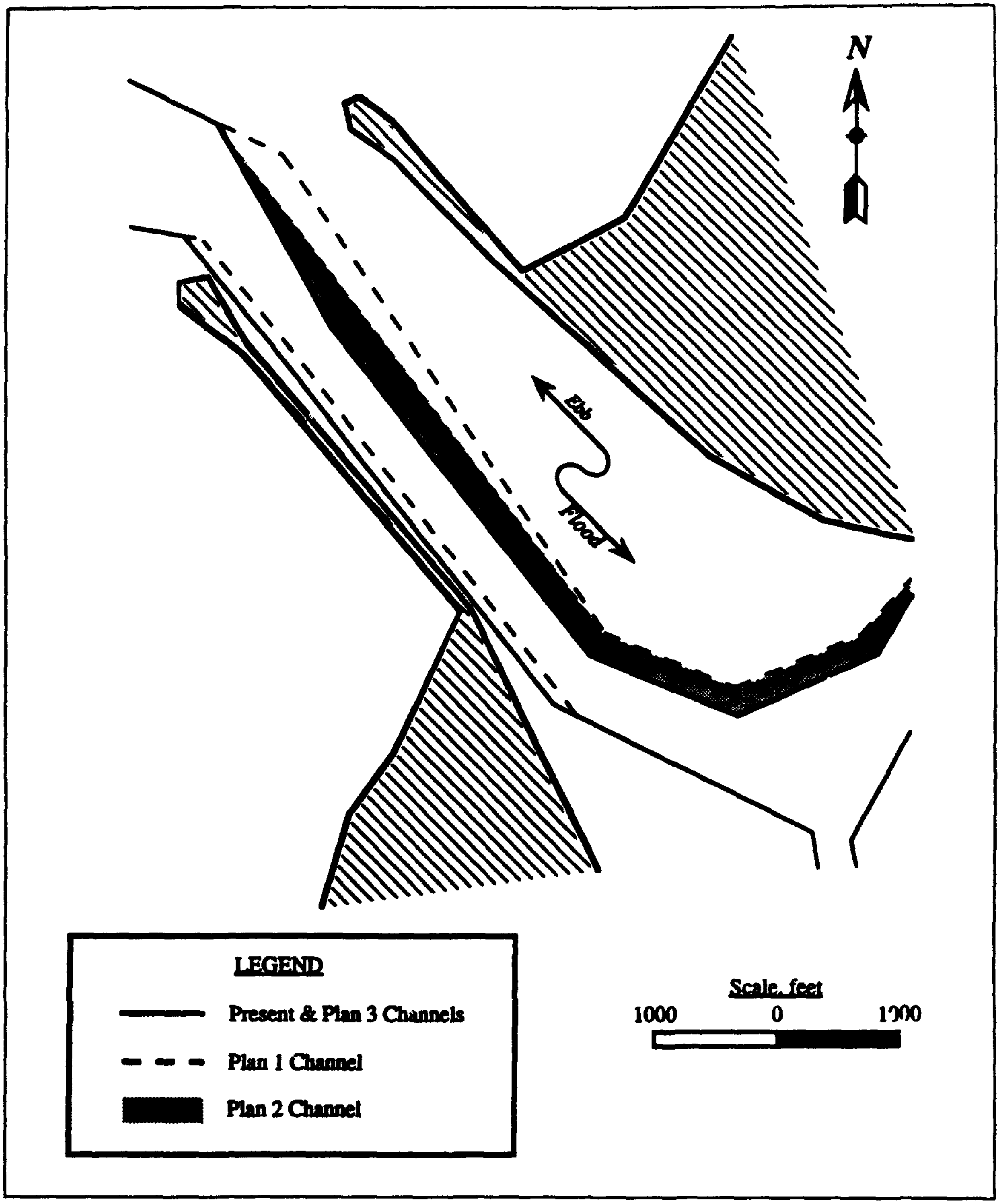

Figure 4. Humboldt Bay Entrance Channel boundaries

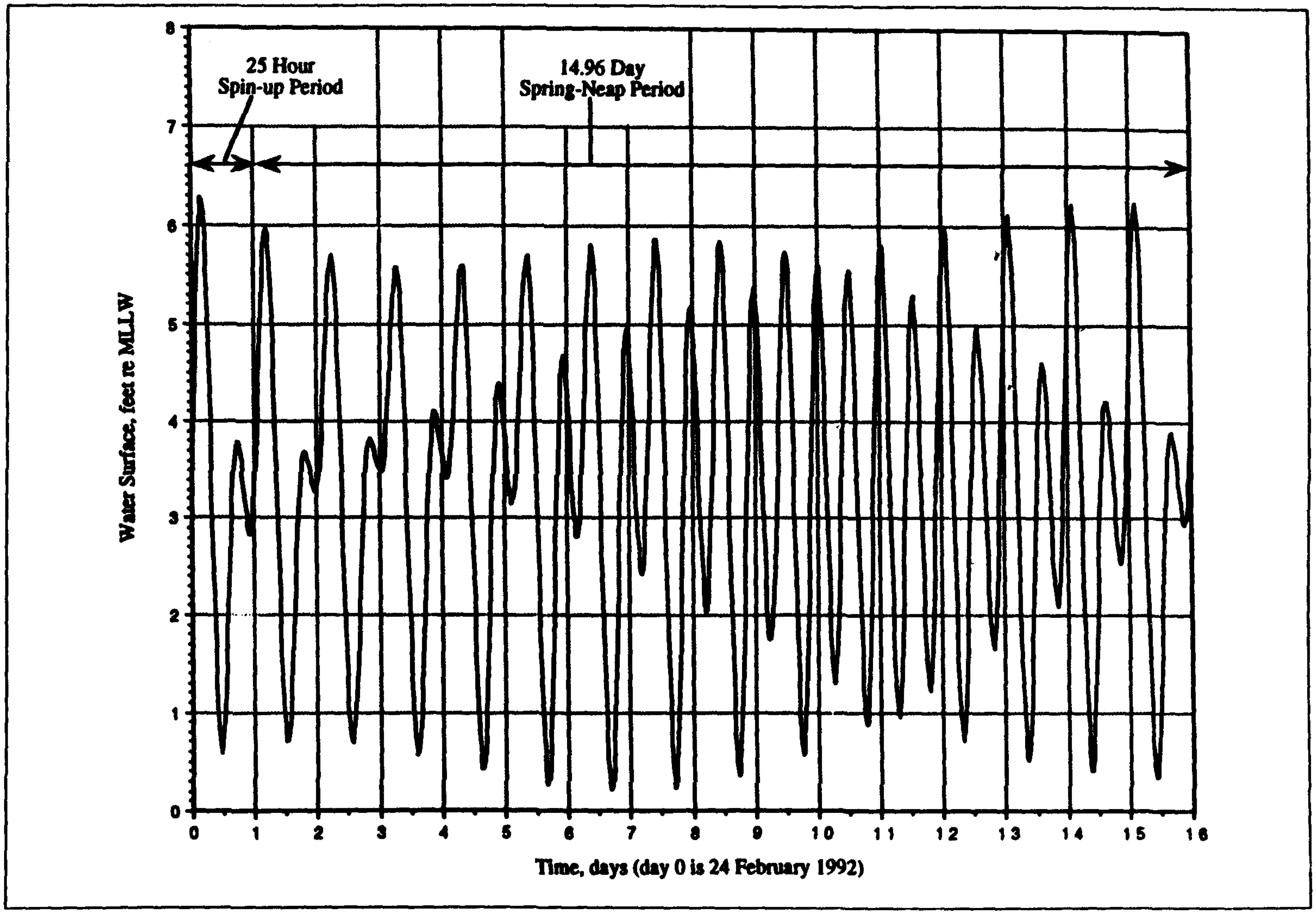

Figure 5. Ocean boundary tide, Humboldt Bay

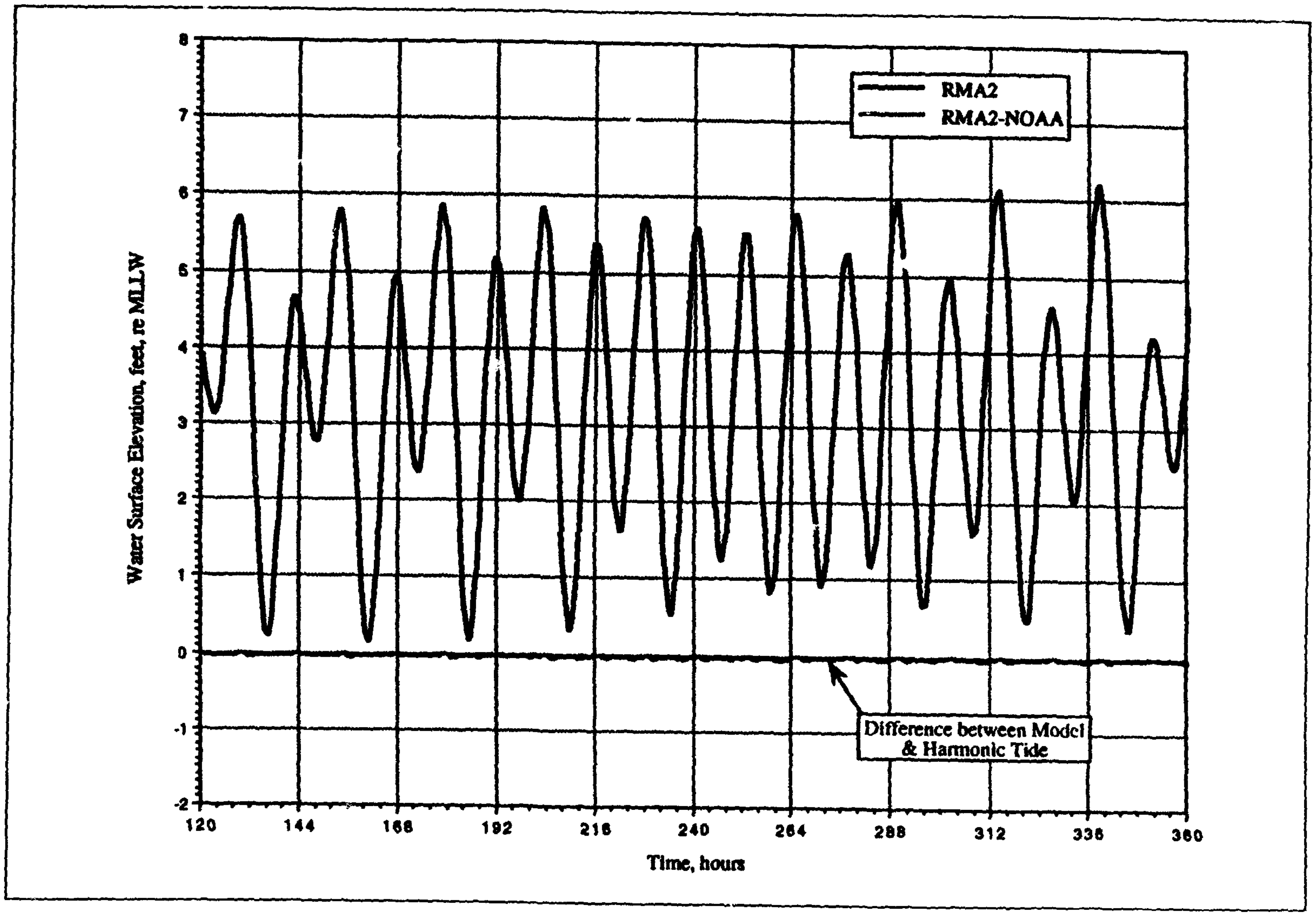

Figure 6. Predicted (RMA-2) tide and difference from NOAA harmonic tide, Entrance Channel

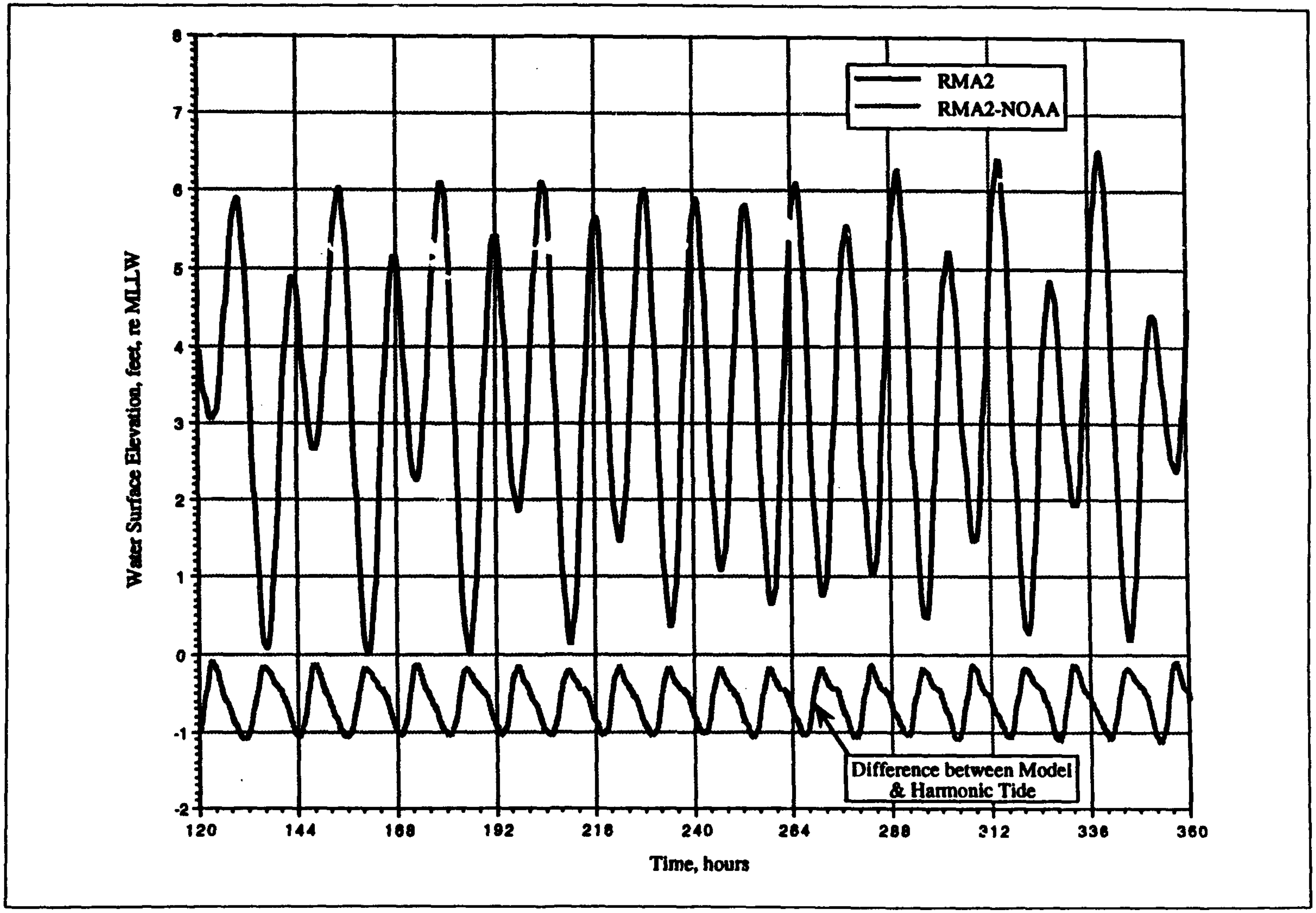

Figure 7. Predicted (RMA-2) tide and difference from NOAA harmonic tide, Eureka Slough Bridge

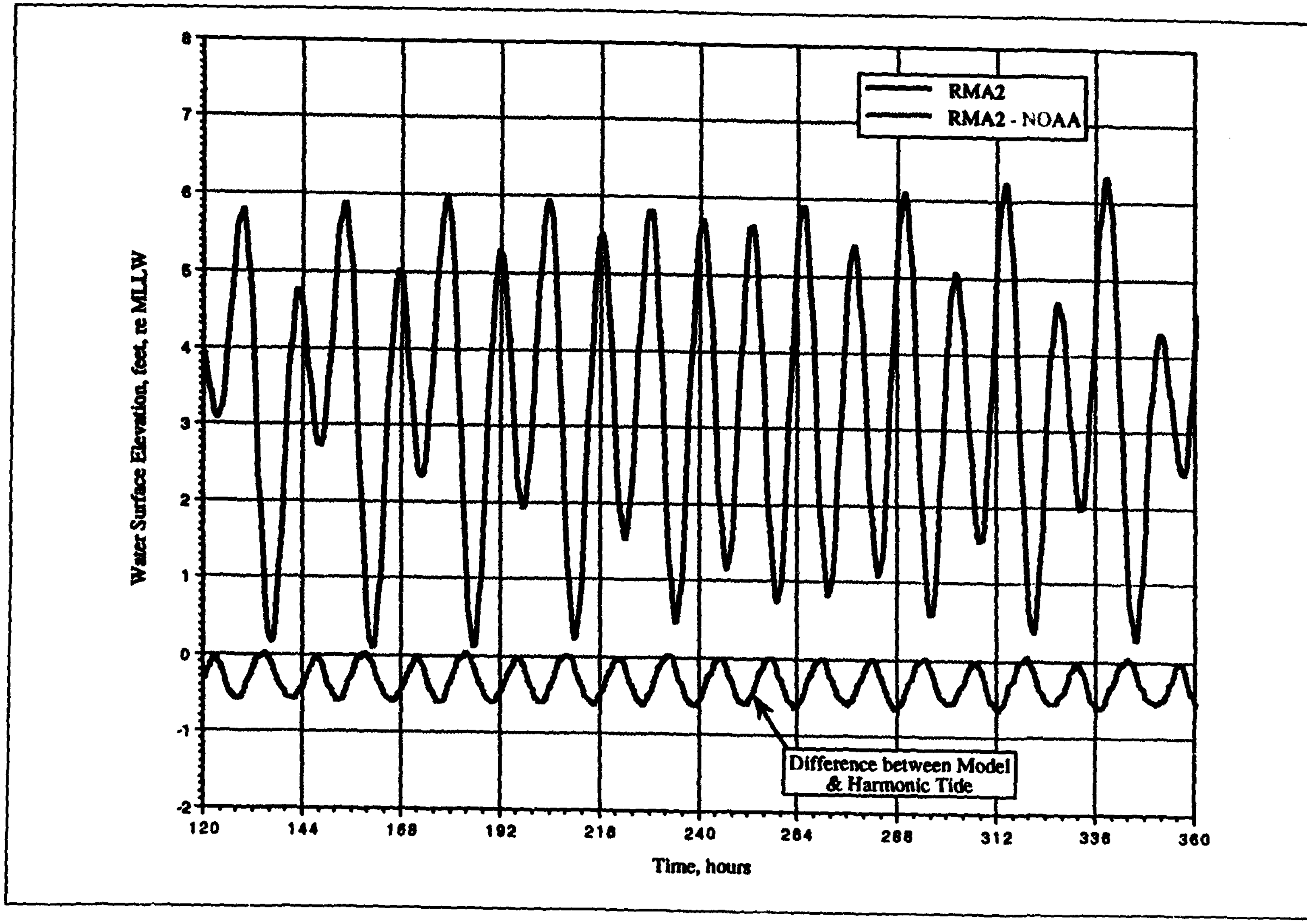

Figure 8. Predicted (RMA-2) tide with difference from NOAA harmonic tide, Fields Landing

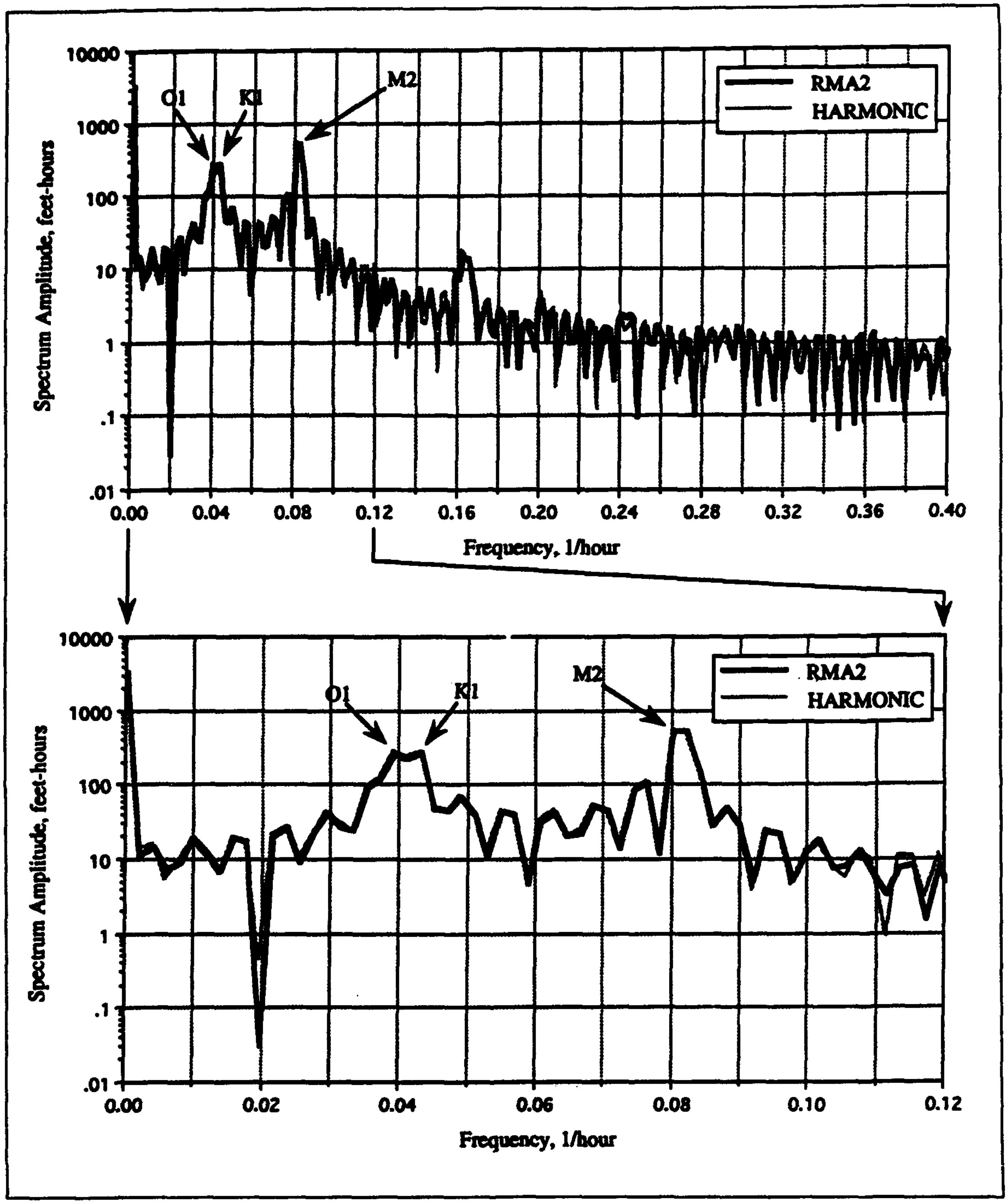

Figure 9. Humboldt Bay Entrance tide spectrum for RMA-2 and harmonic tide

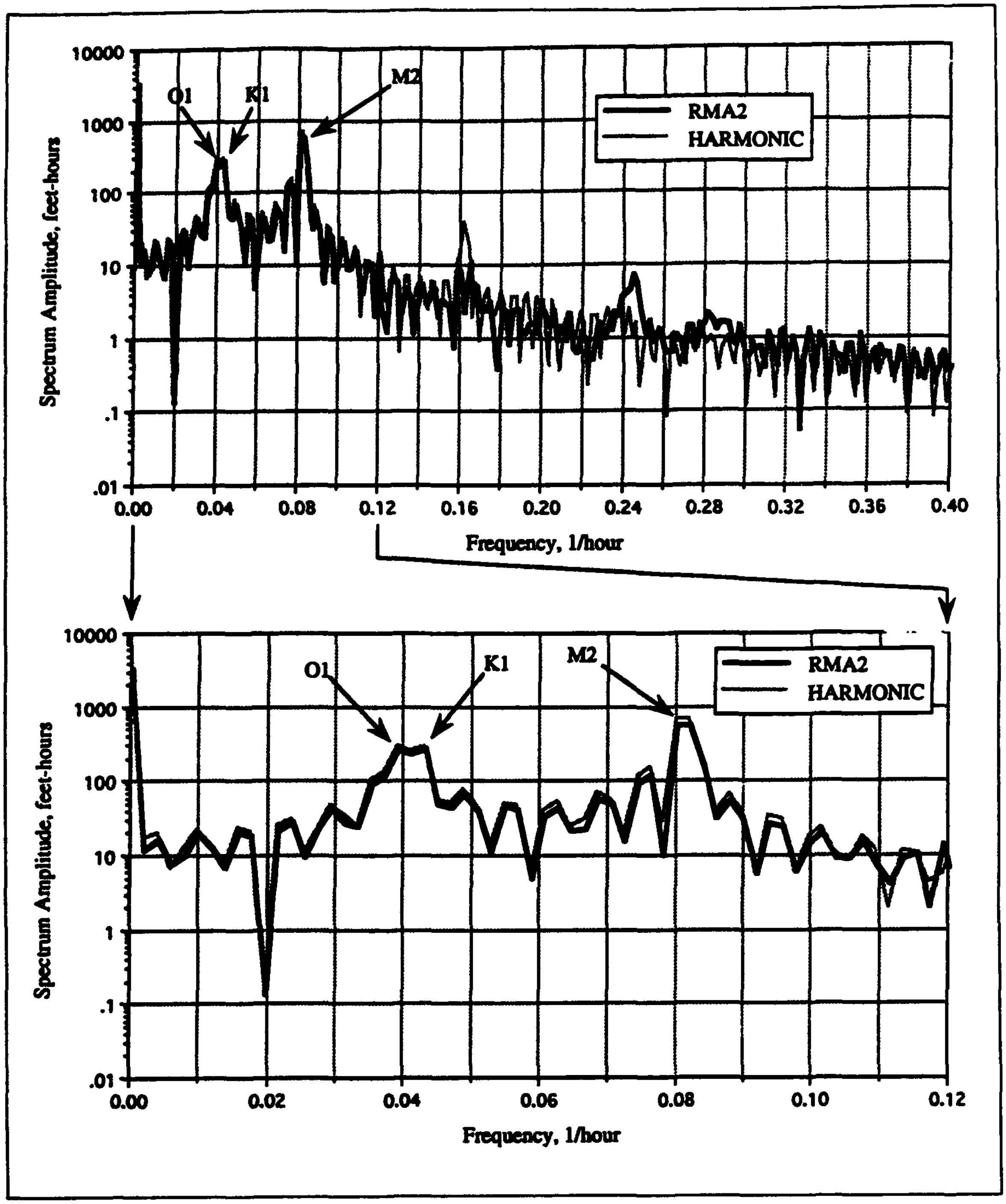

Figure 10. Eureka Slough Bridge tide spectrum for RMA-2 and harmonic tide

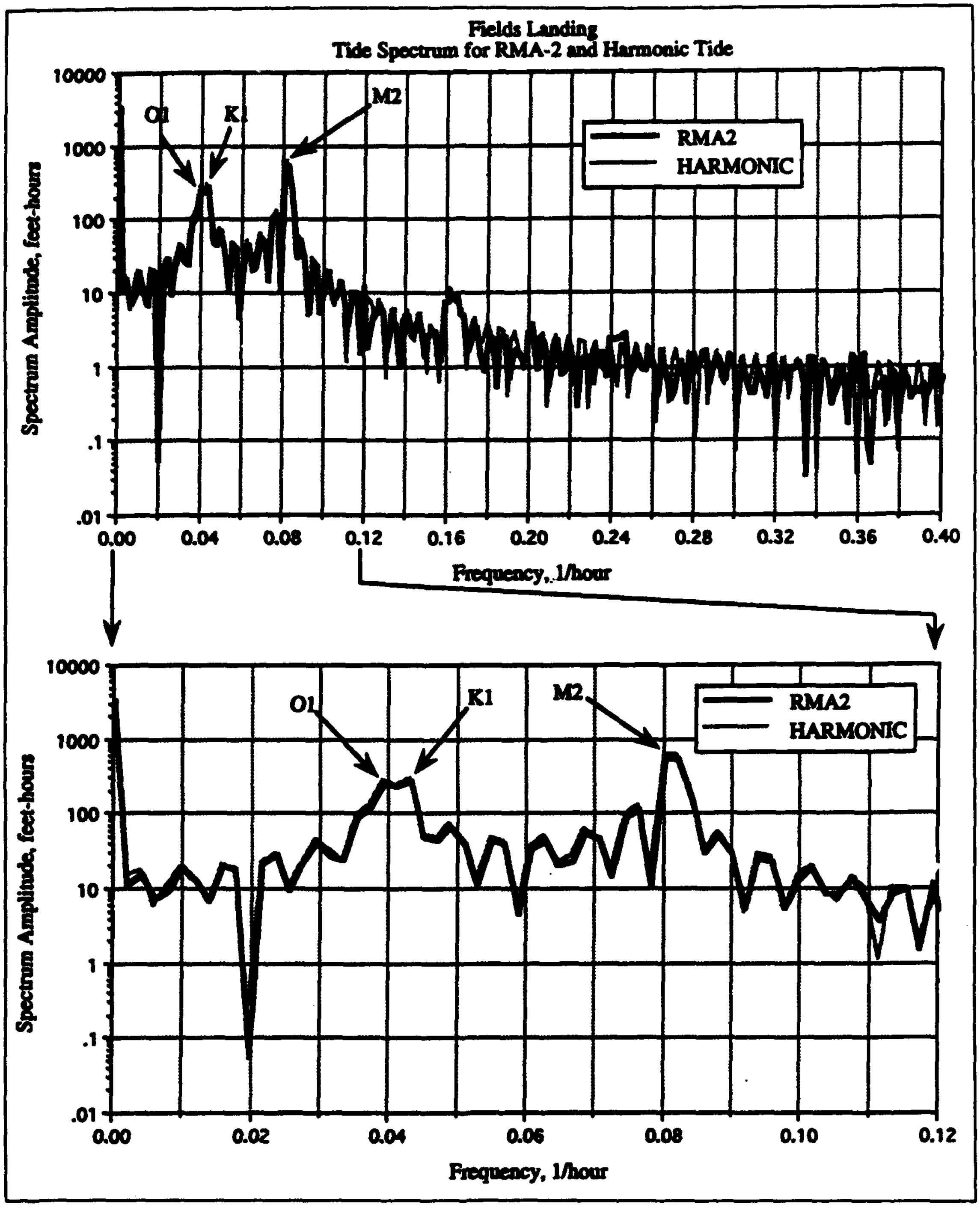

Figure 11. Fields Landing tide spectrum for RMA-2 and harmonic tide

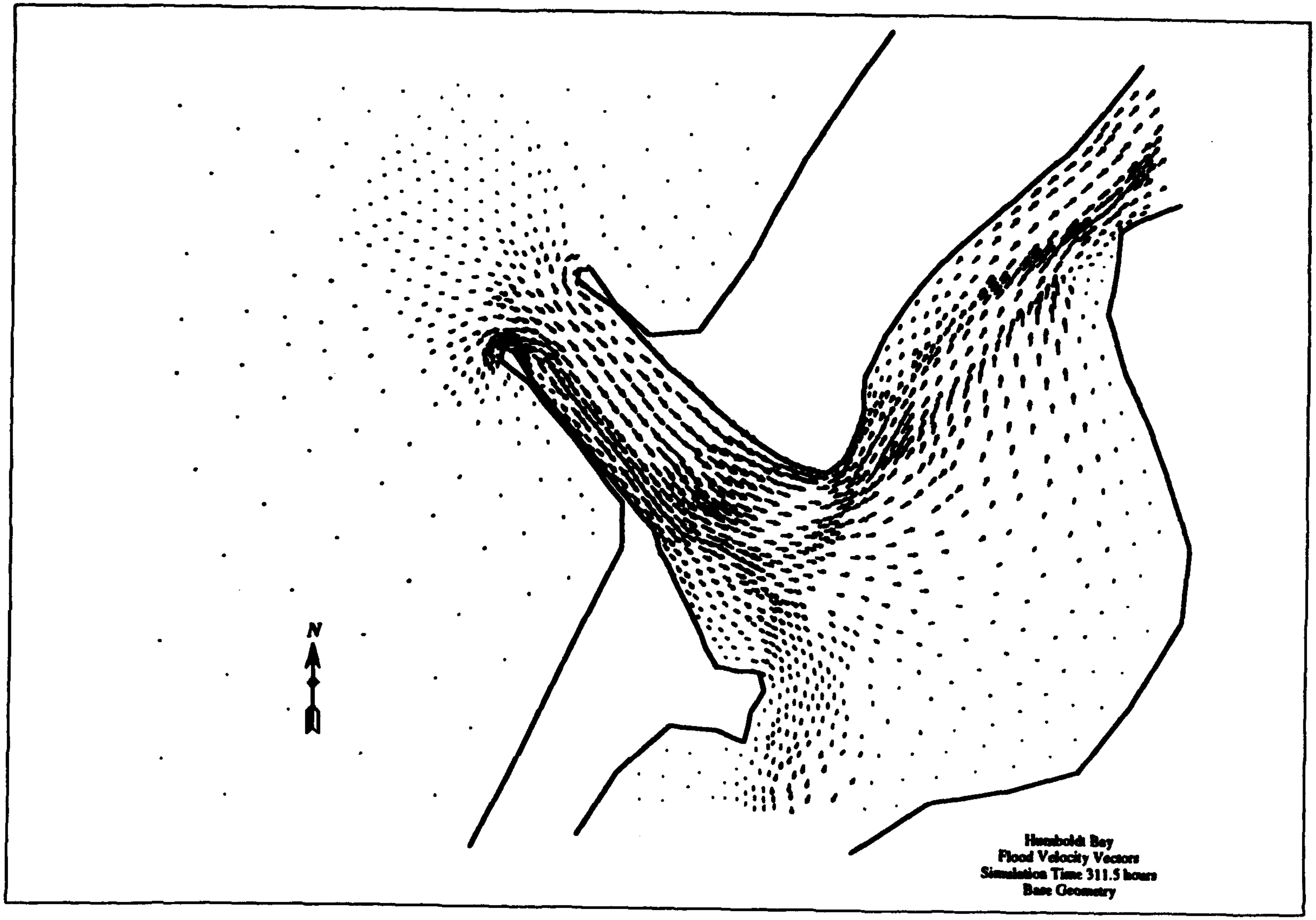

Figure 12. Base water velocity vectors, flood

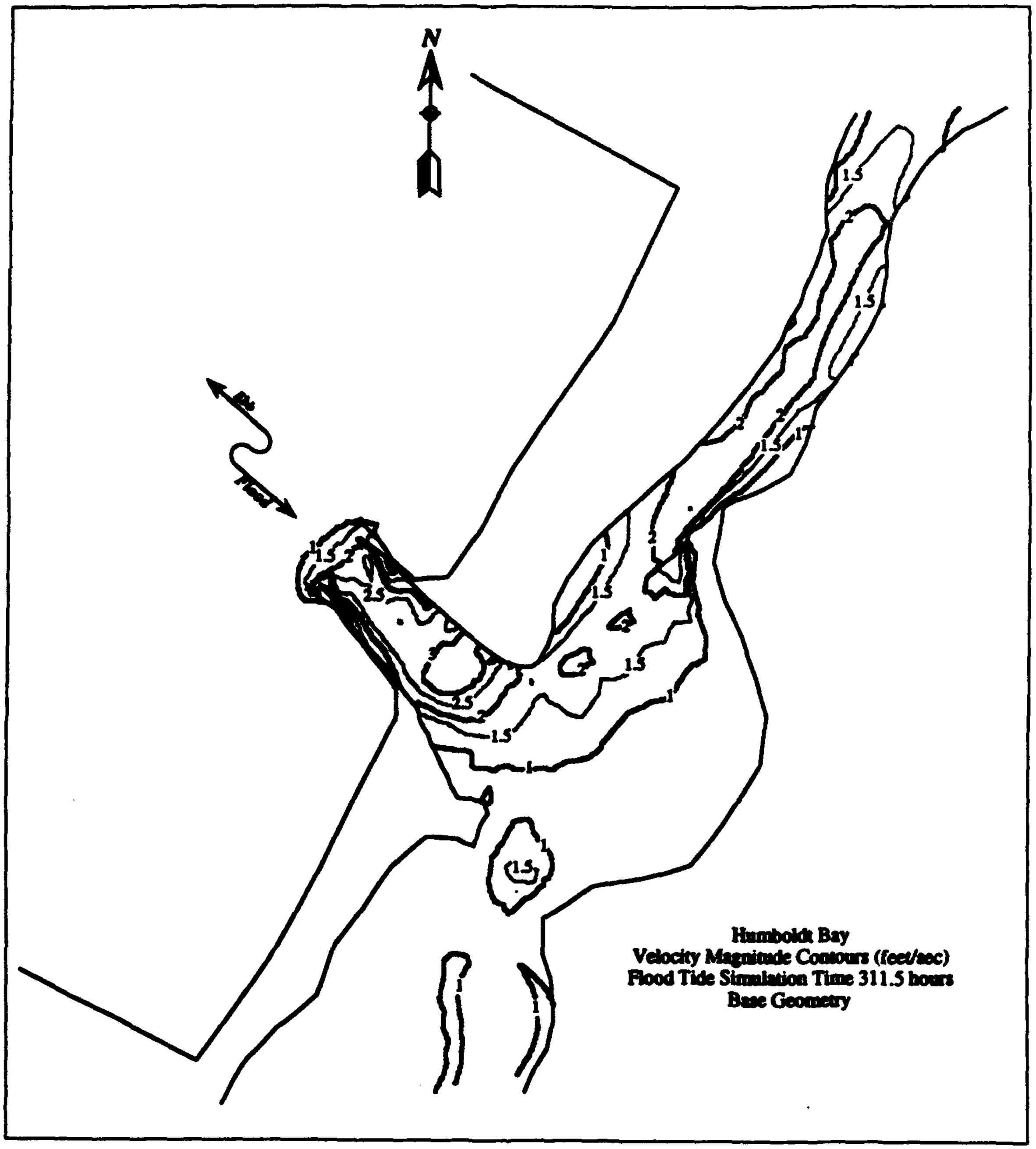

Figure 13. Base water velocity contours, flood

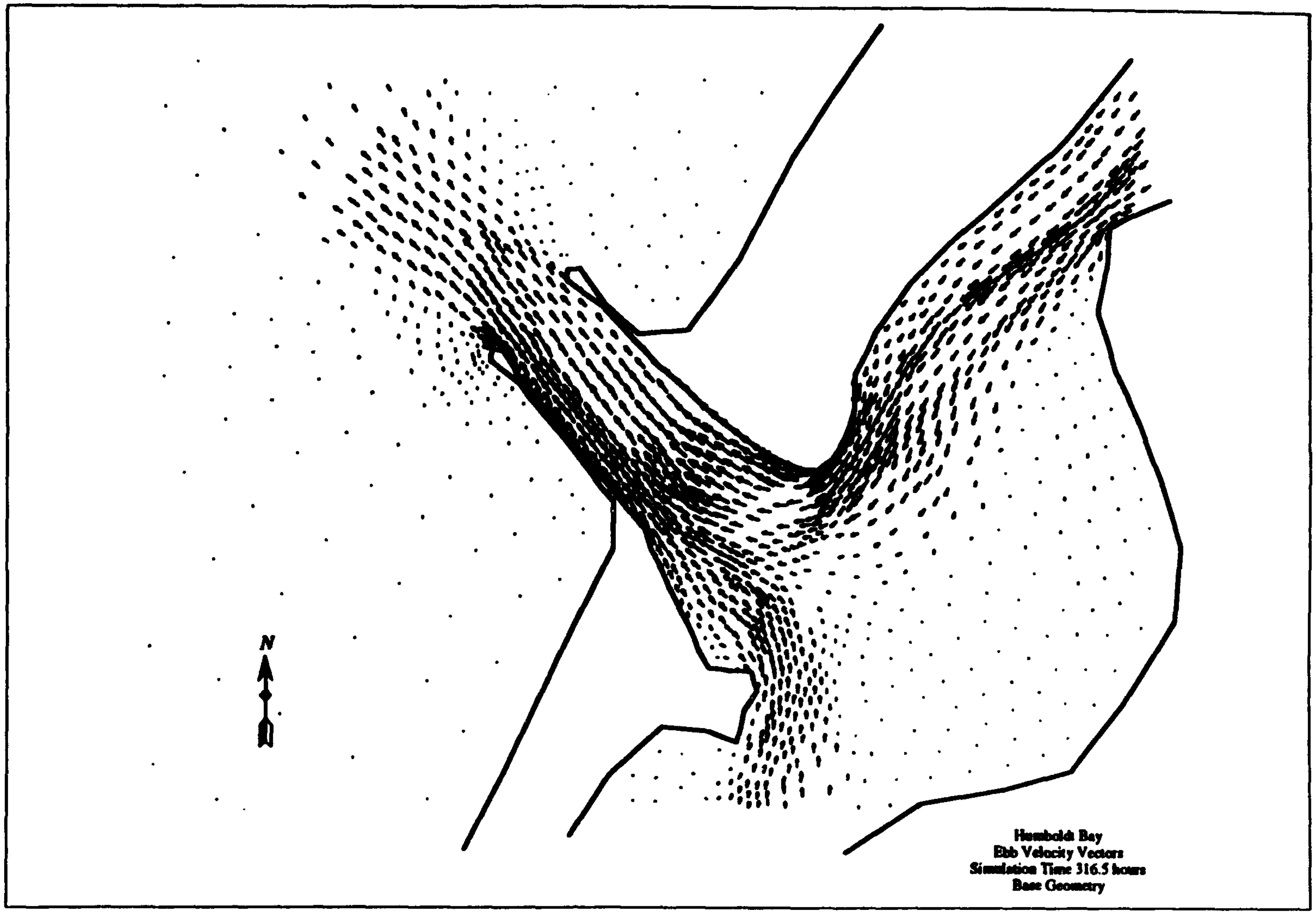

Figure 14. Base water velocity vectors, ebb

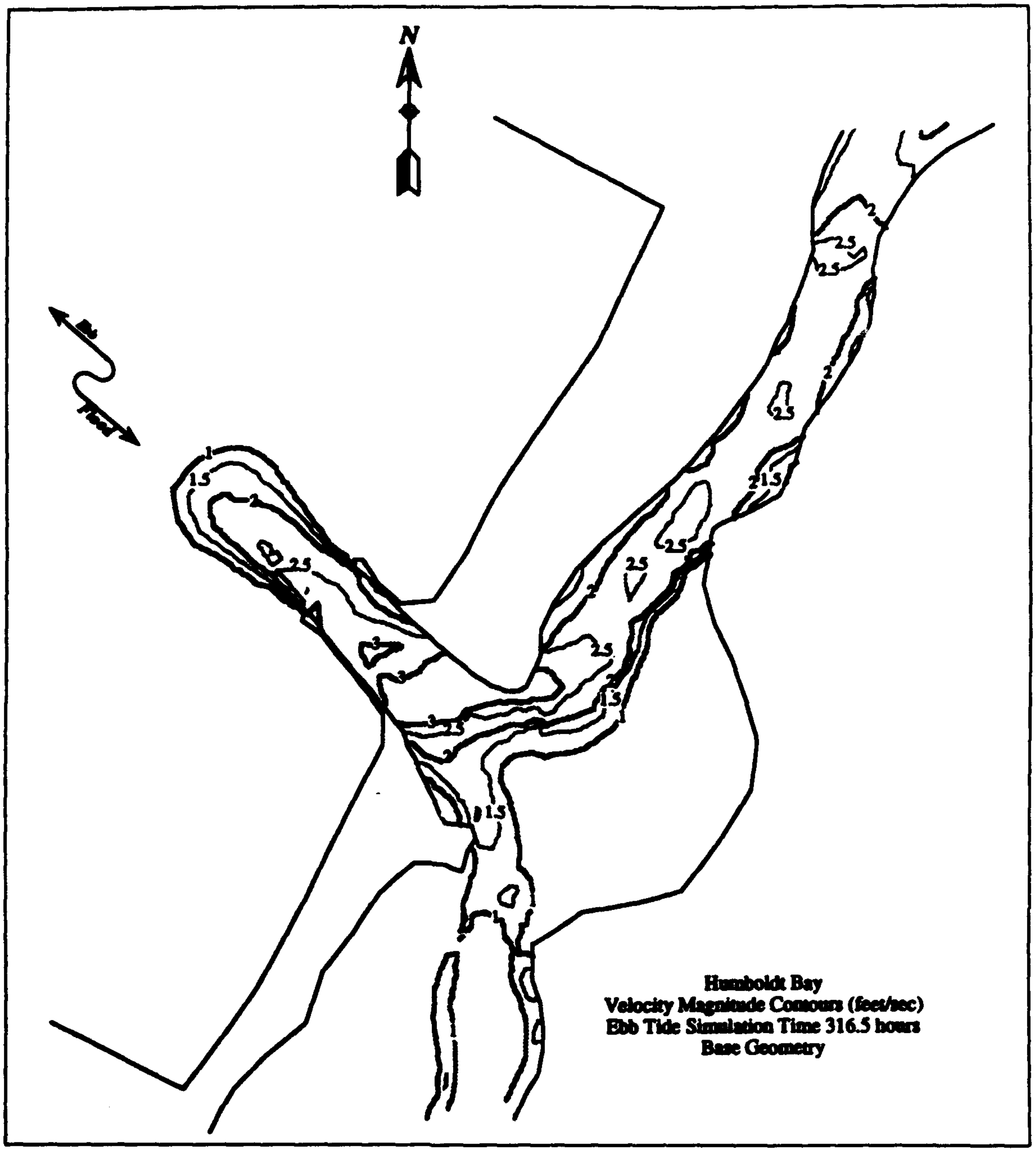

Figure 15. Base water velocity contours, ebb

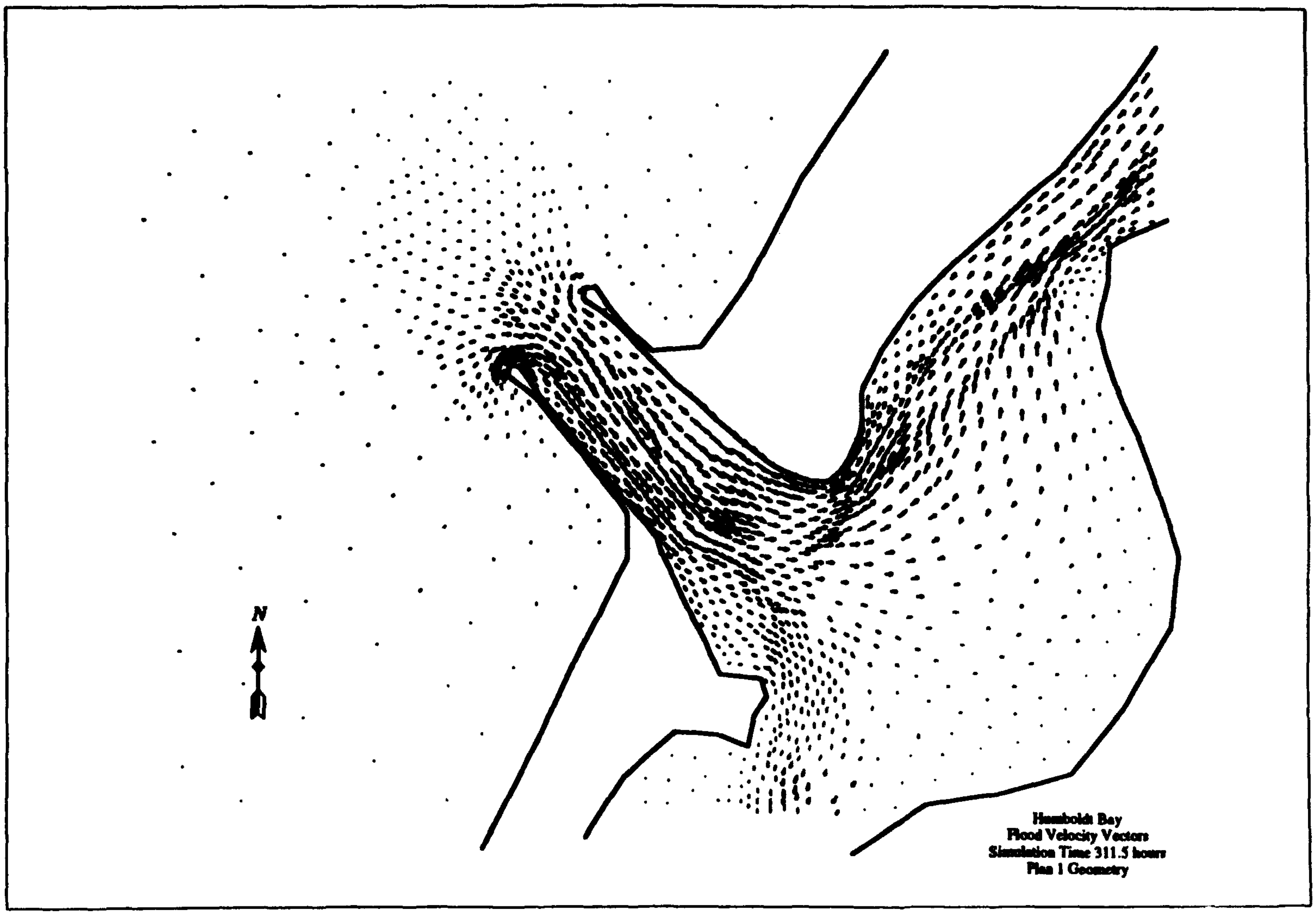

Figure 16. Plan 1 water velocity vectors, flood

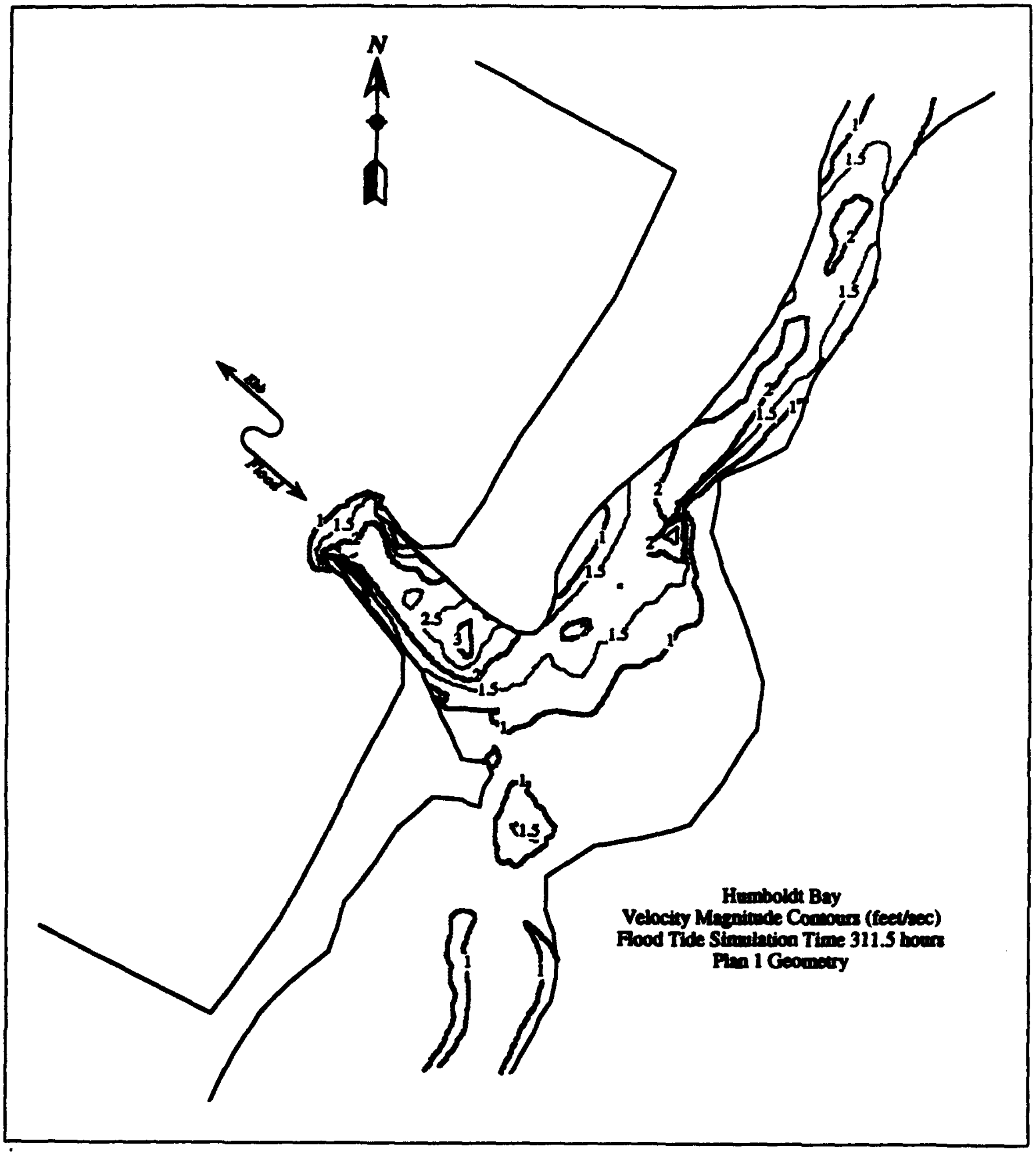

Figure 17. Plan 1 water velocity contours, flood

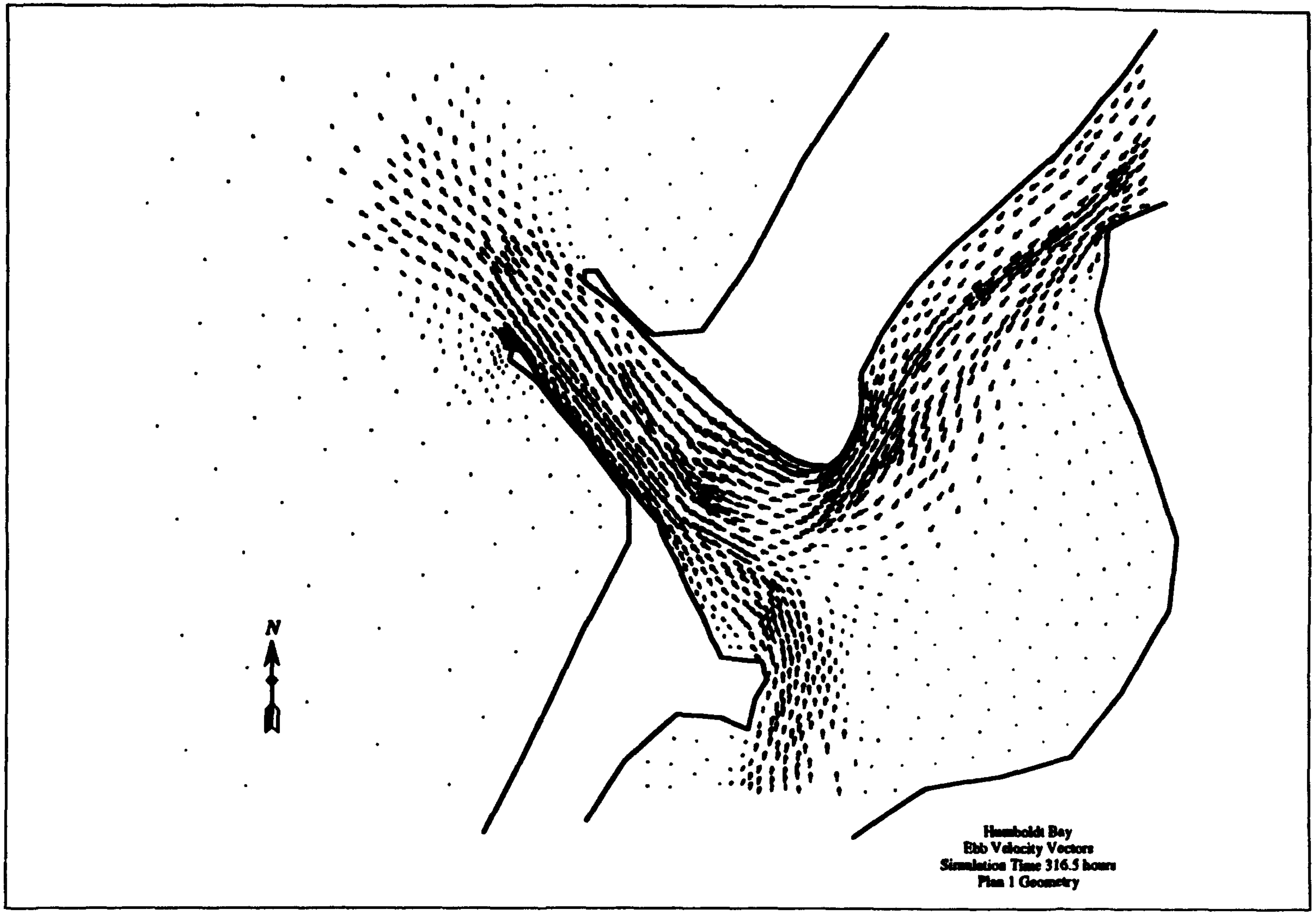

Figure 18. Plan 1 water velocity vectors, ebb

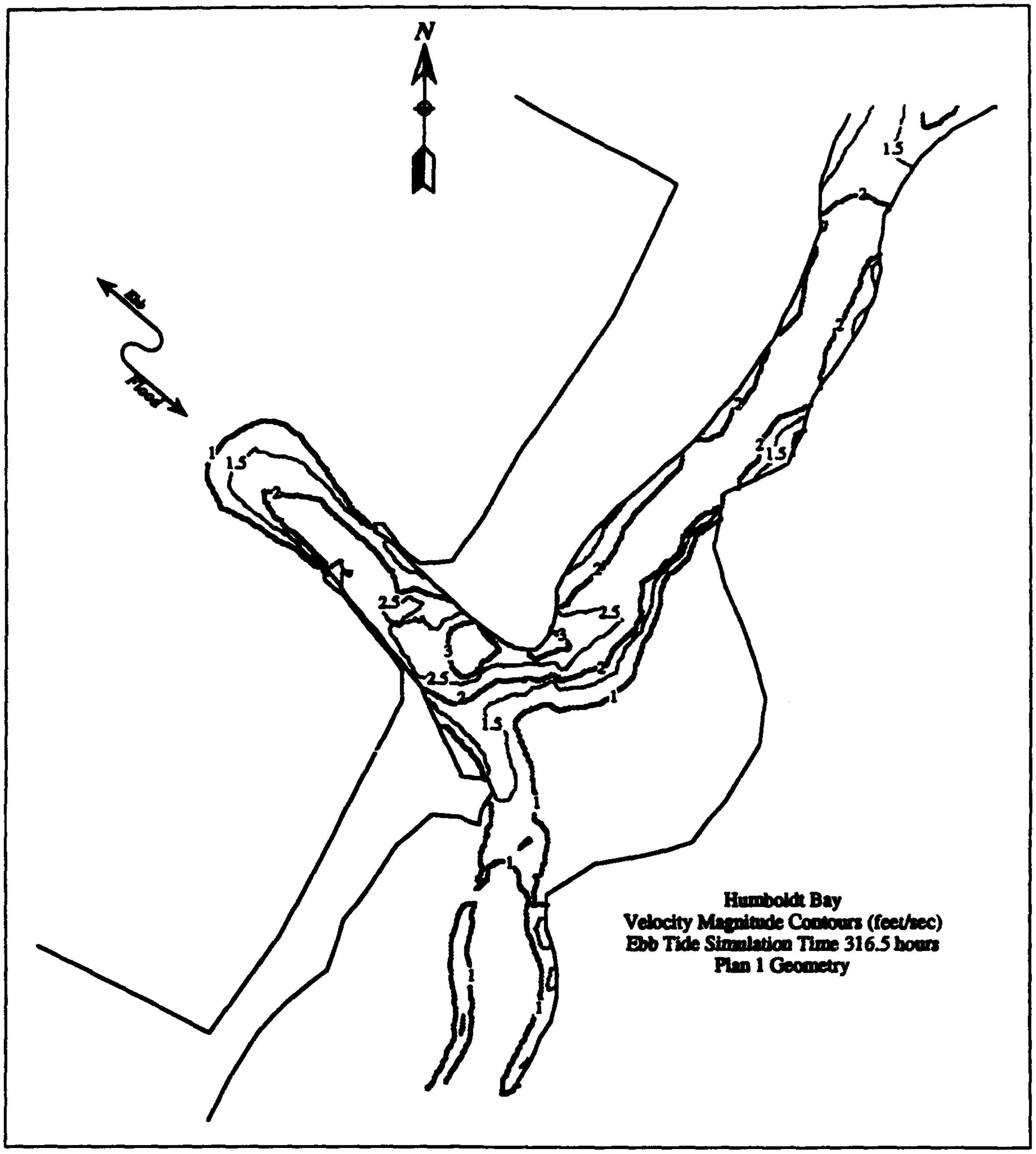

Figure 19. Plan 1 water velocity contours, ebb

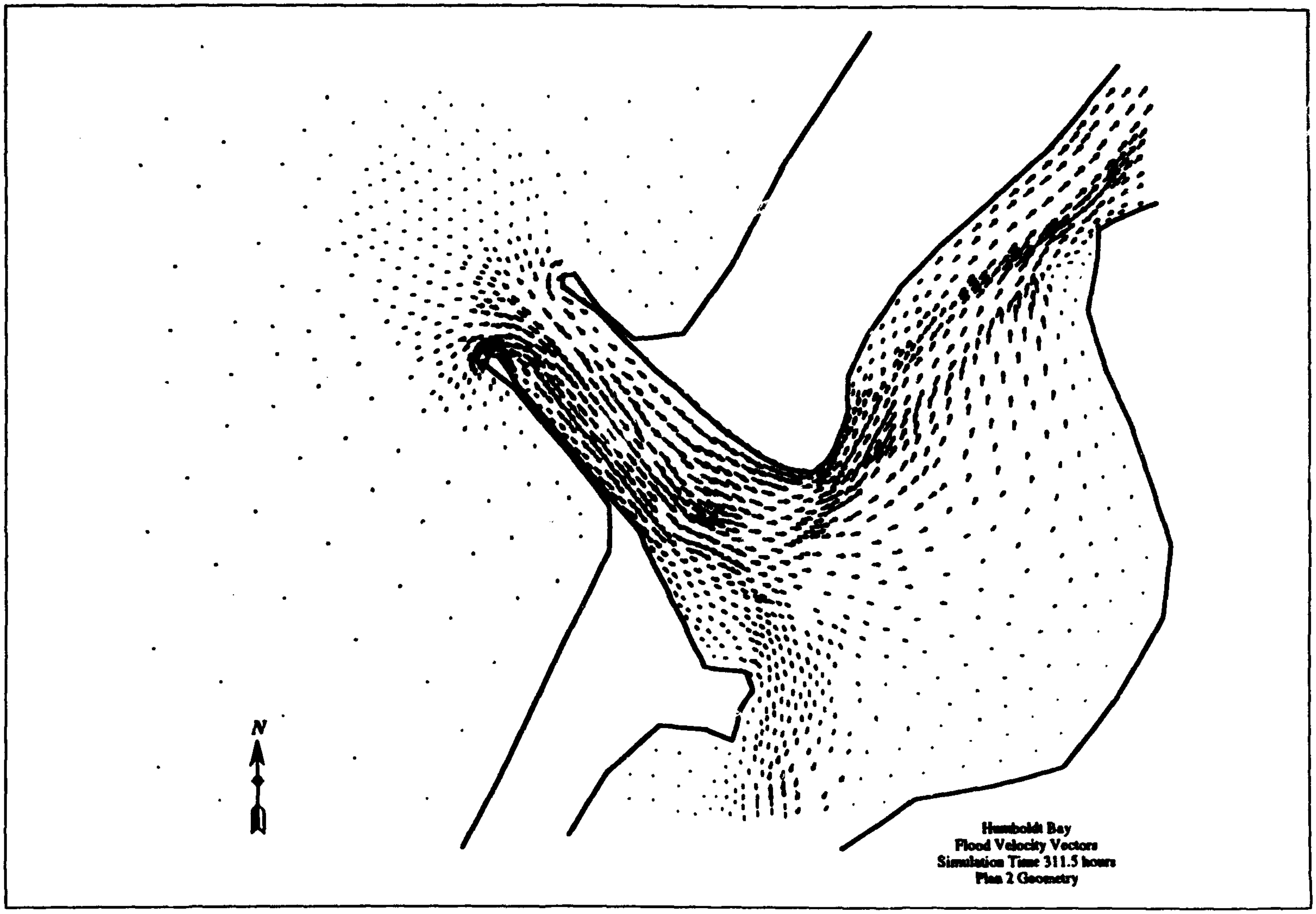

Figure 20. Plan 2 water velocity vectors, flood

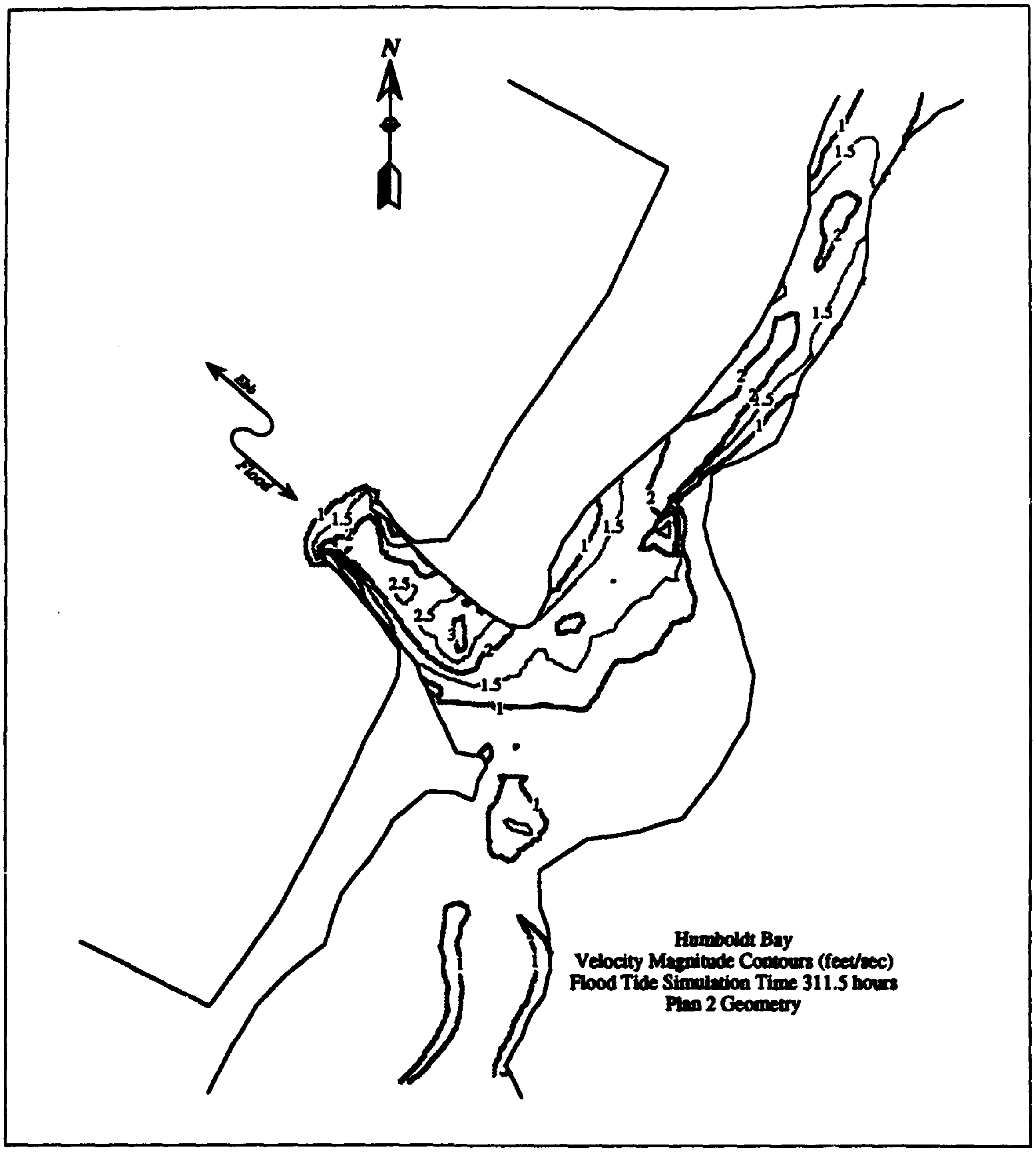

Figure 21. Plan 2 water velocity contours, flood

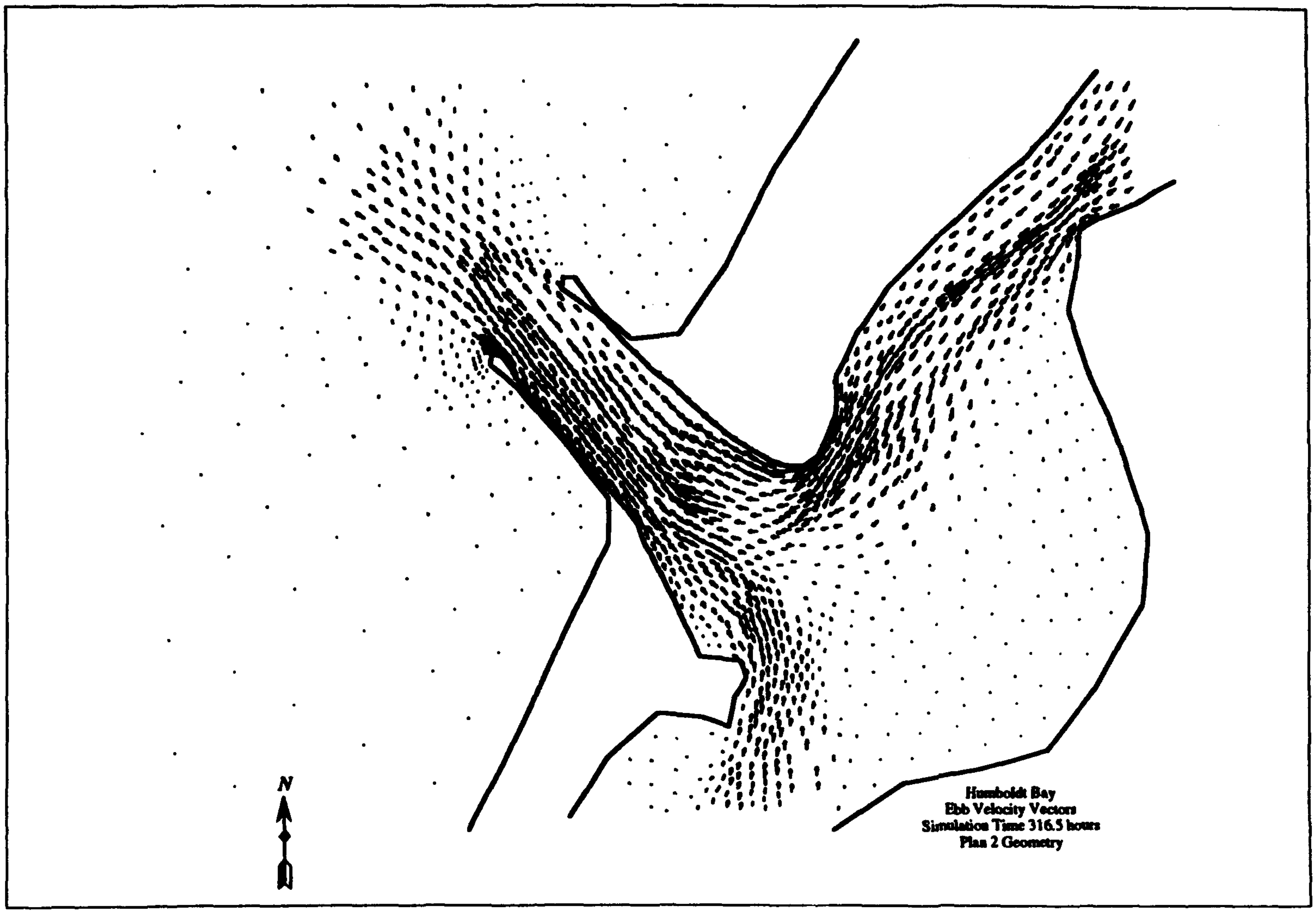

Figure 22. Plan 2 water velocity vectors, ebb

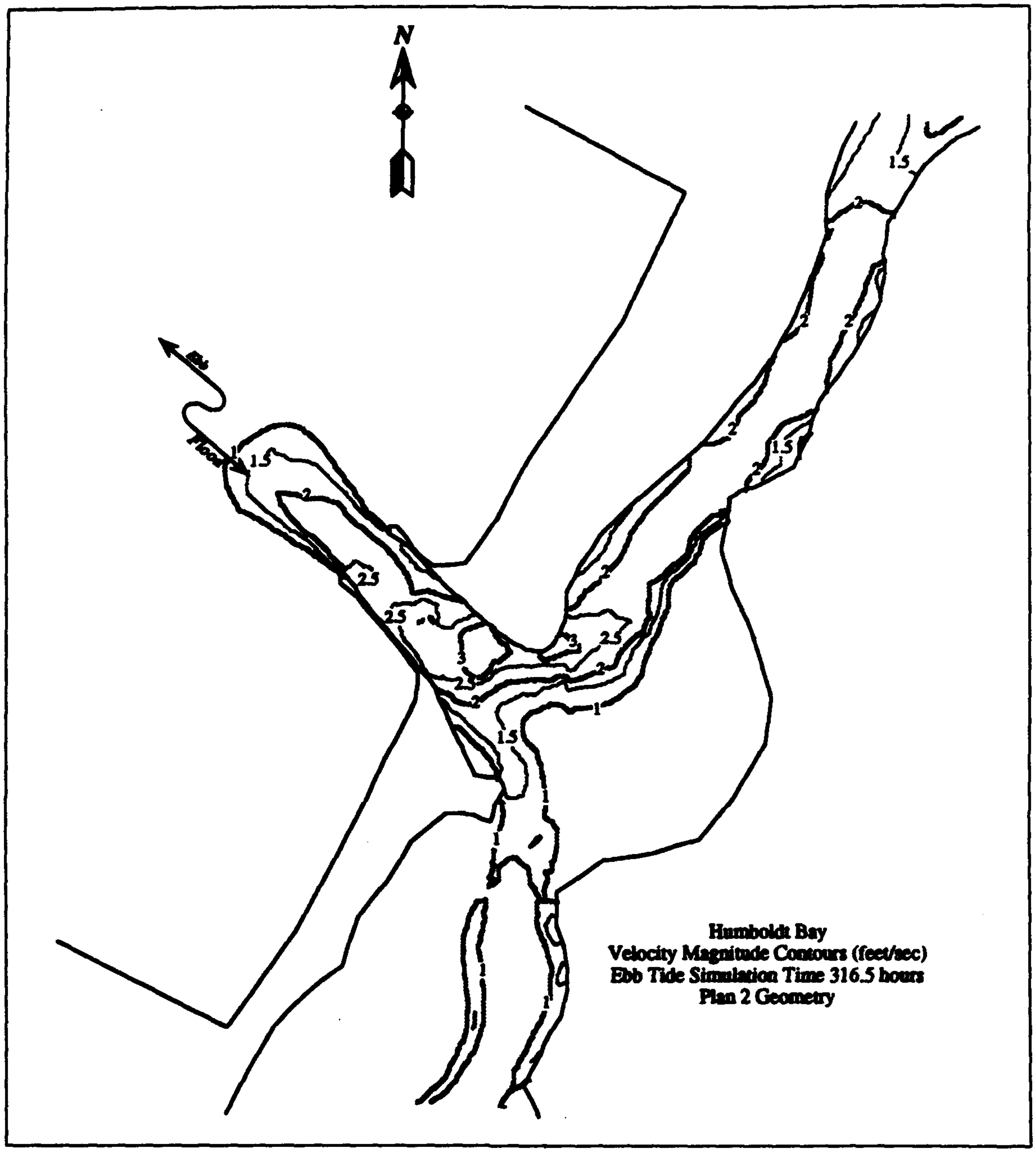

Figure 23. Plan 2 water velocity contours, ebb

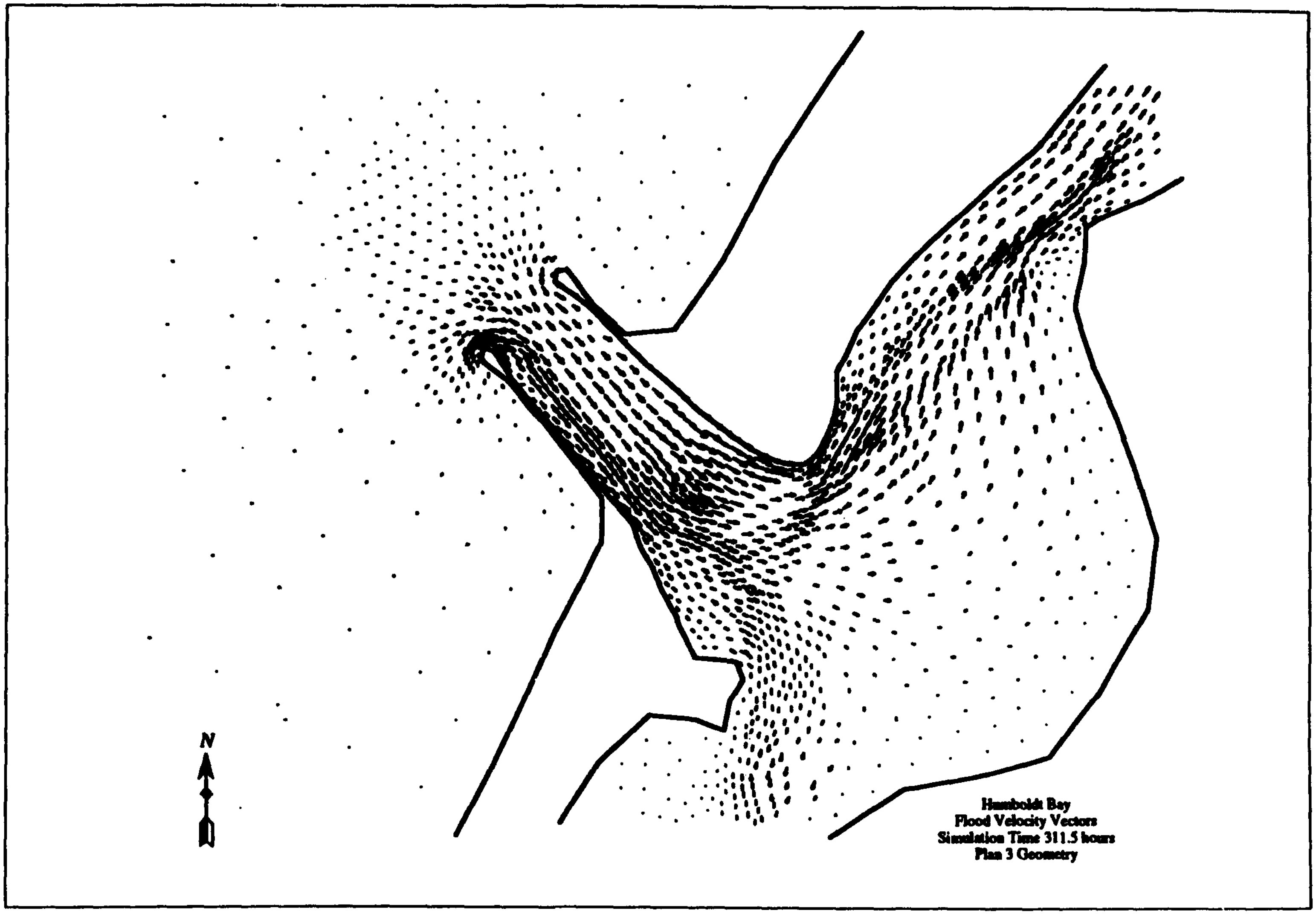

Figure 24. Plan 3 water velocity vectors, flood

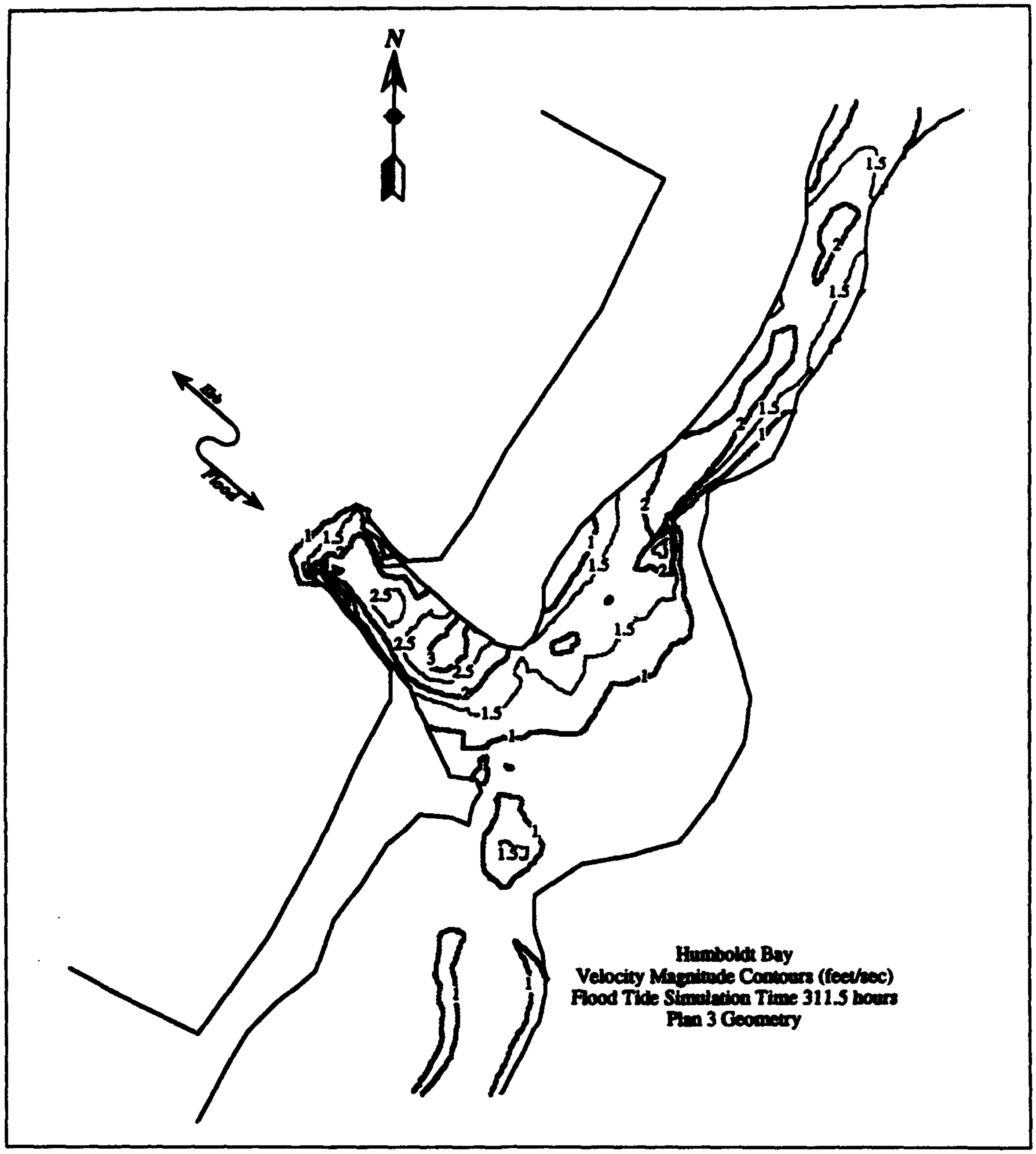

Figure 25. Plan 3 water velocity contours, flood

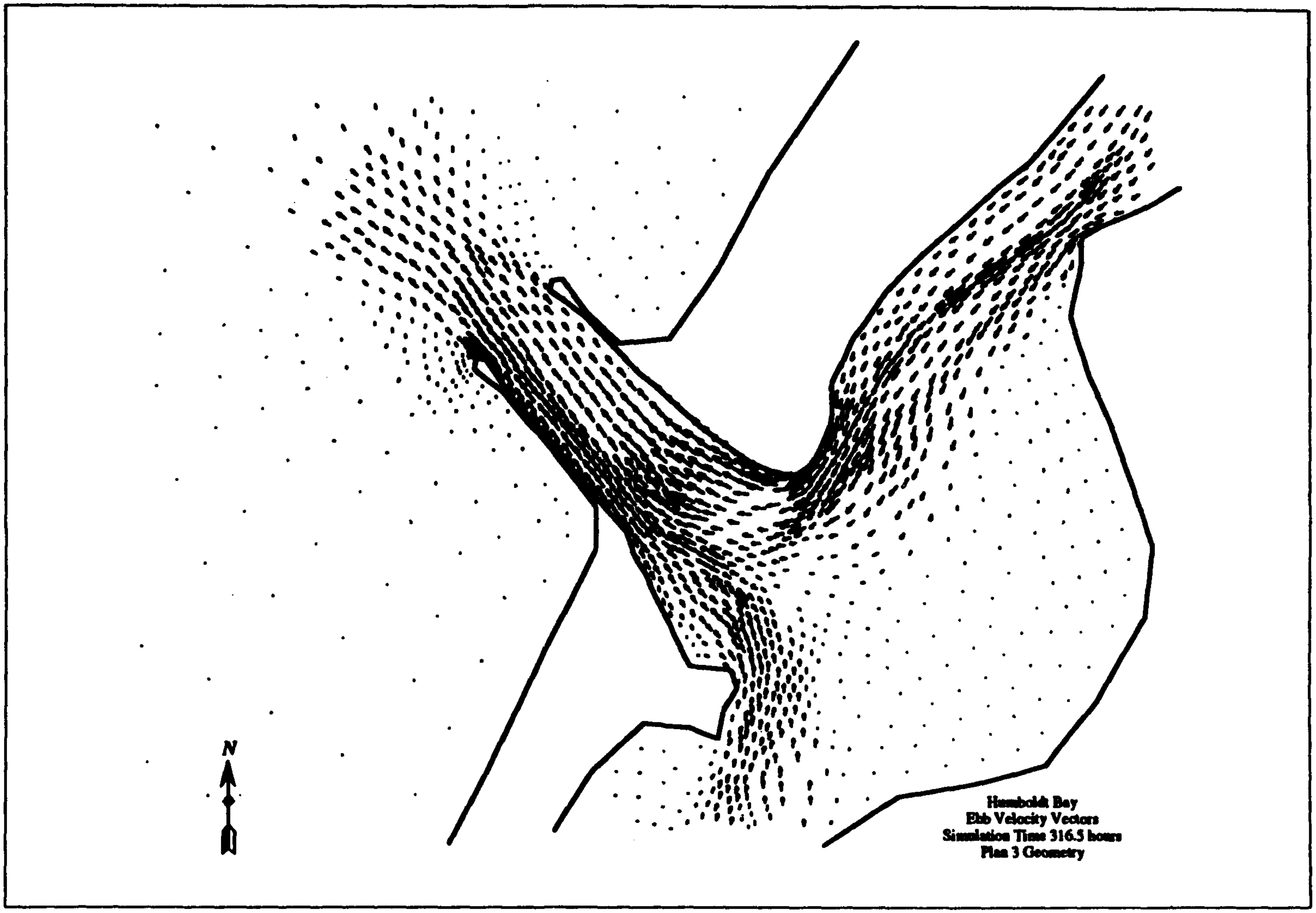

Figure 26. Plan 3 water velocity vectors, ebb

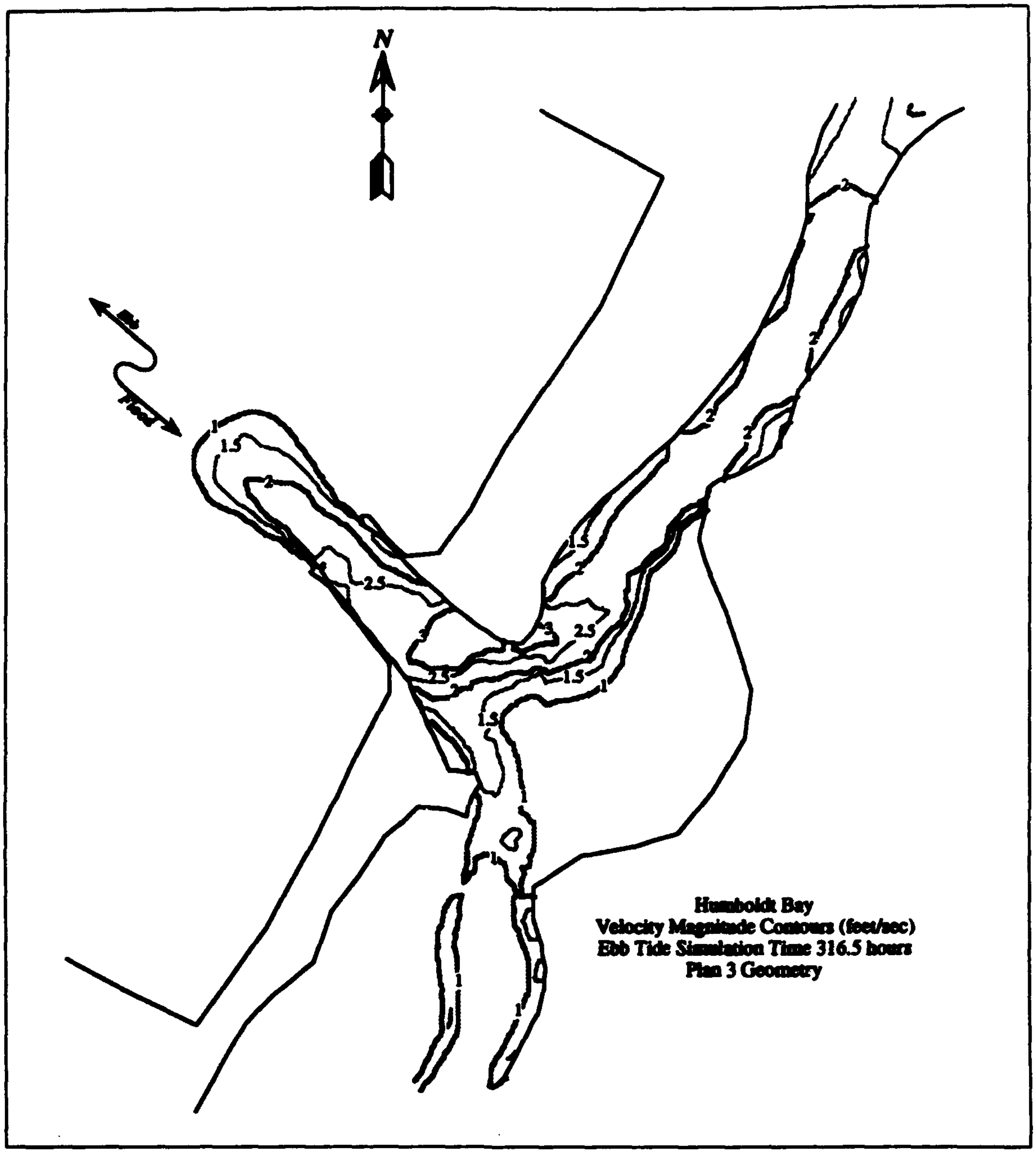

Figure 27. Plan 3 water velocity contours, ebb

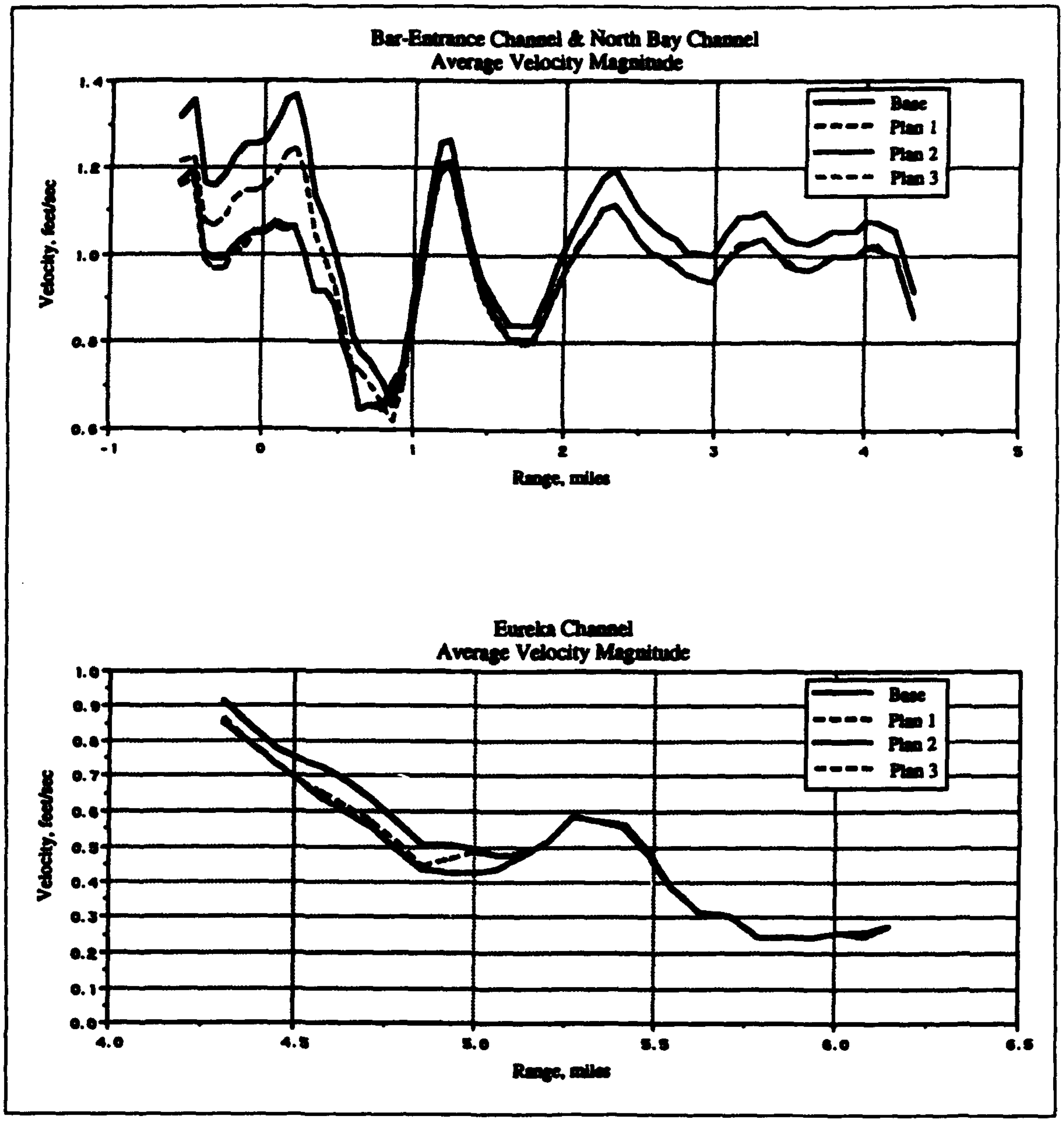

Figure 28. Average velocity magnitudes, Entrance, North Bay, and Eureka Channels

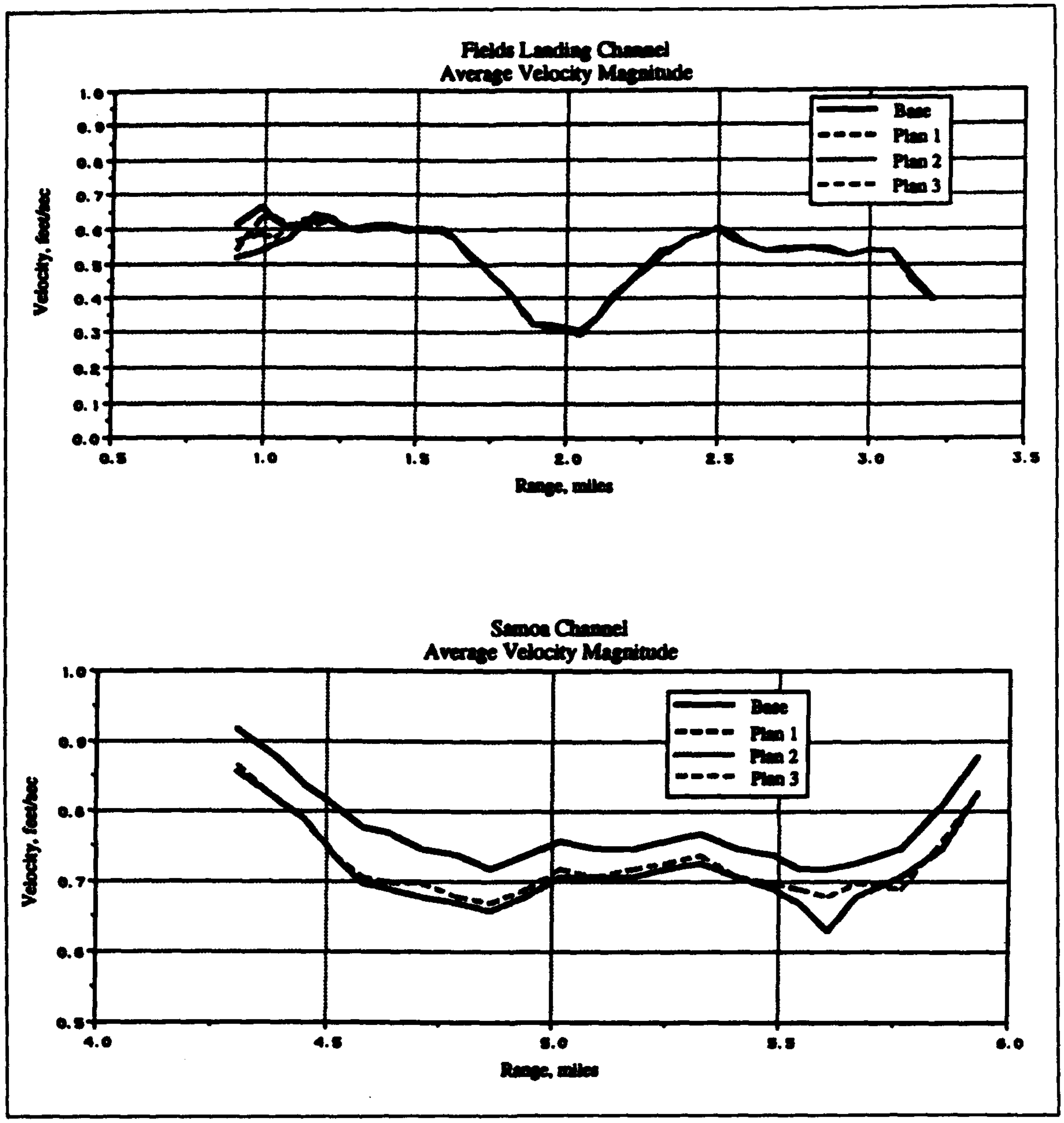

Figure 29. Average velocity magnitudes, Fields Landing and Samoa Channels

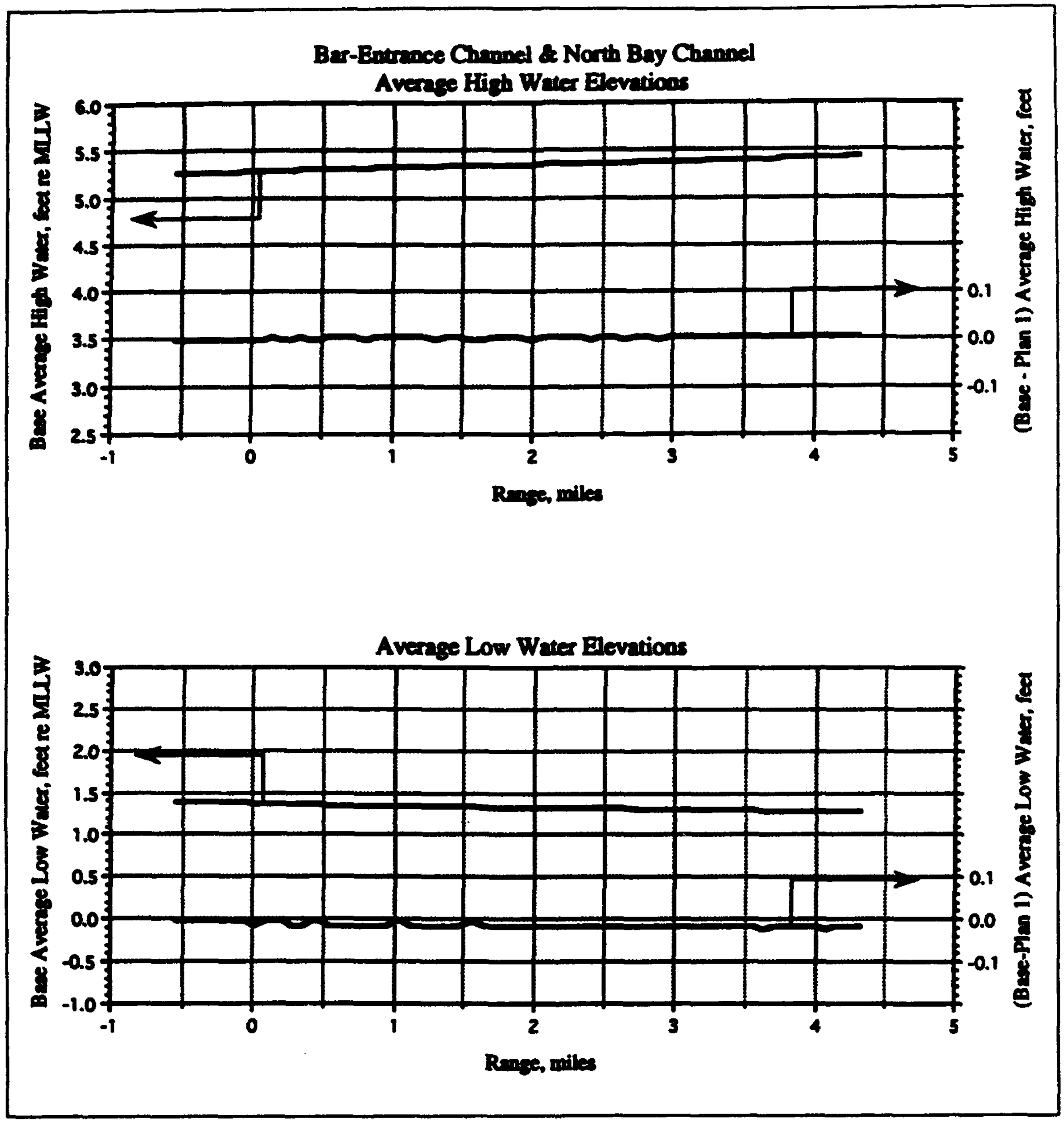

Figure 30. Average high and low water elevations, Base-Plan 1, Bar-Entrance and North Bay Channels

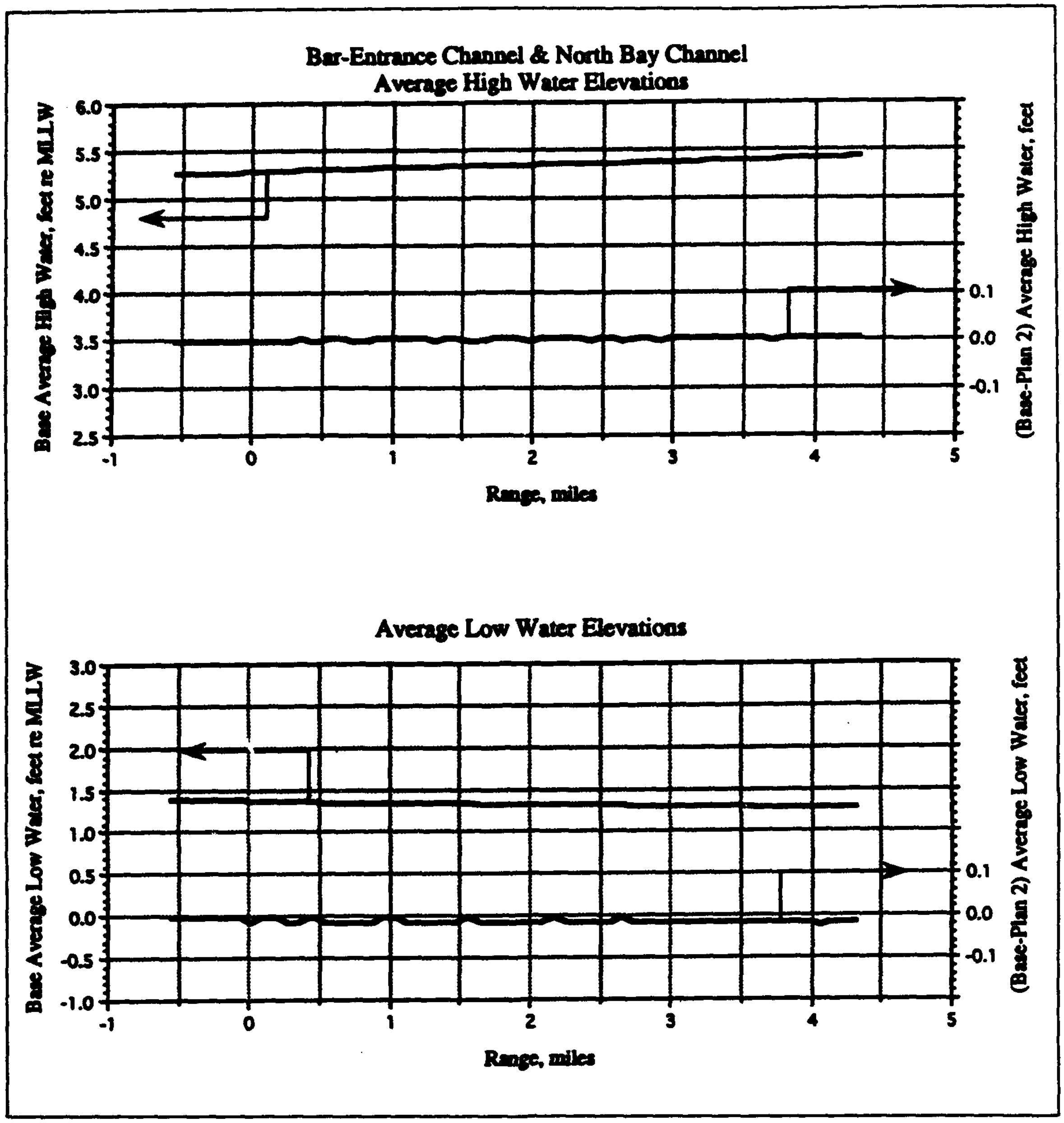

Figure 31. Average high and low water elevations, Base-Plan 2, Bar-Entrance and North Bay Channels

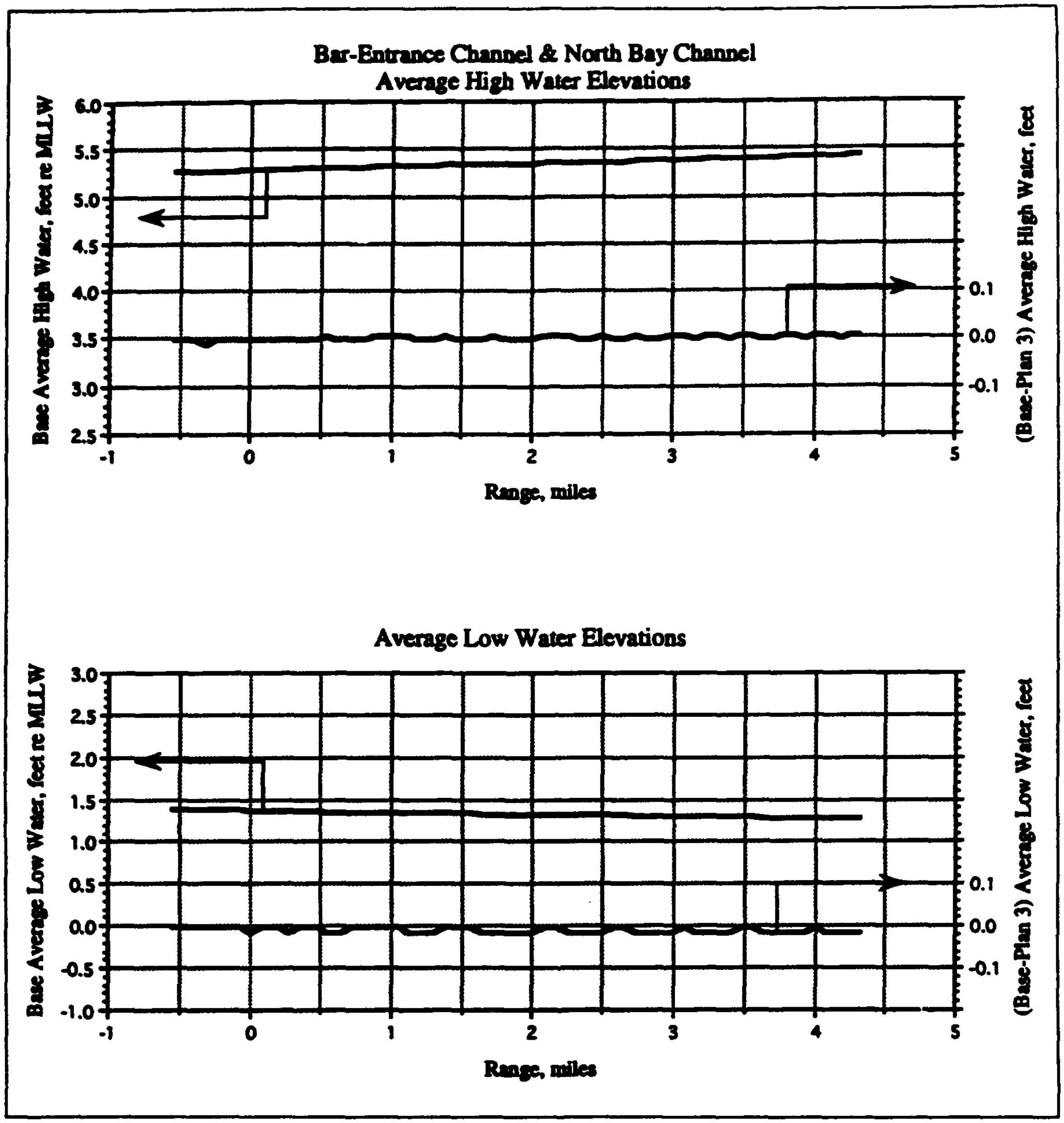

Figure 32. Average high and low water elevations, Base-Plan 3, Bar-Entrance and North Bay Channels

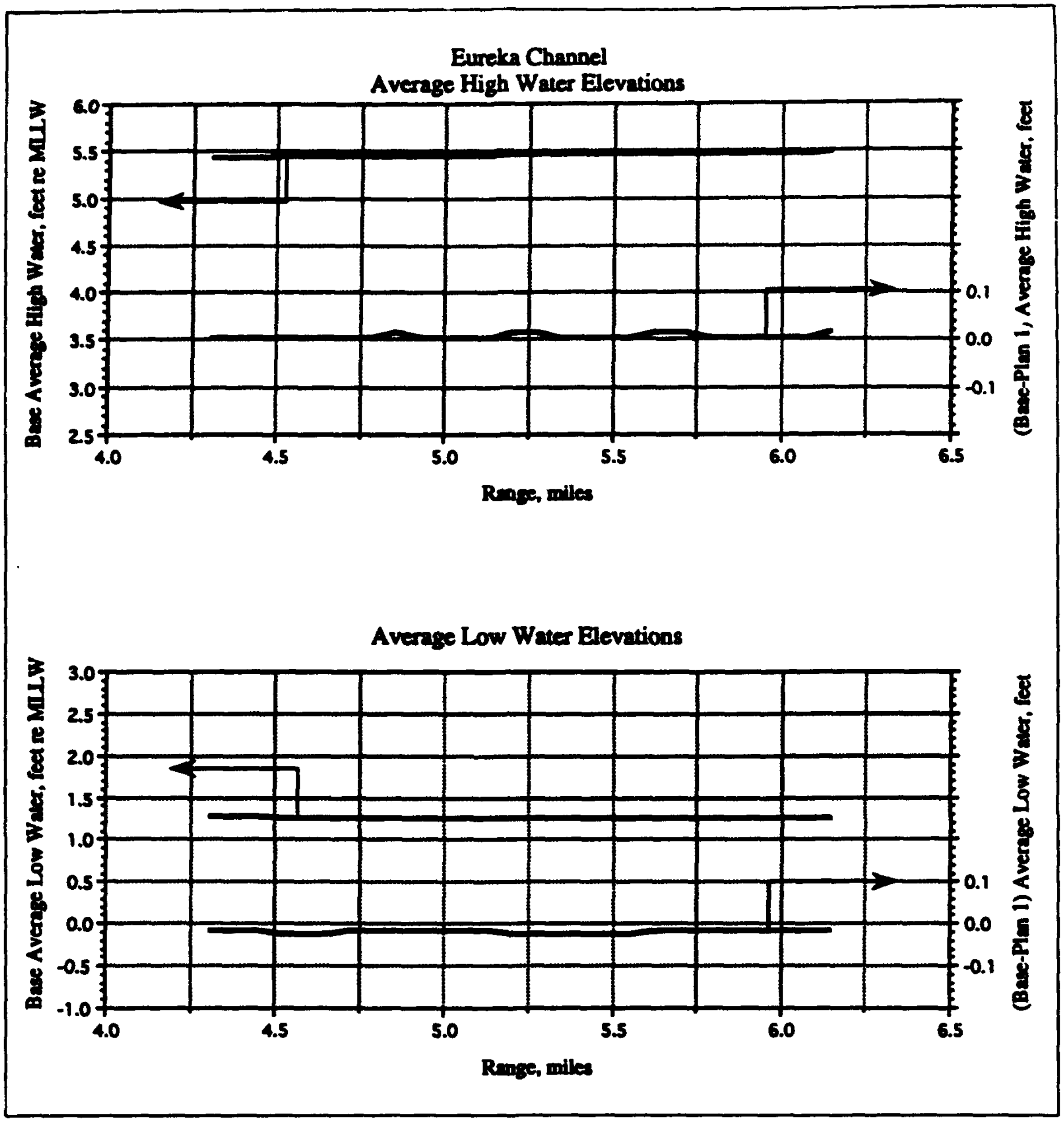

Figure 33. Average high and low water elevations, Base-Plan 1, Eureka Channel

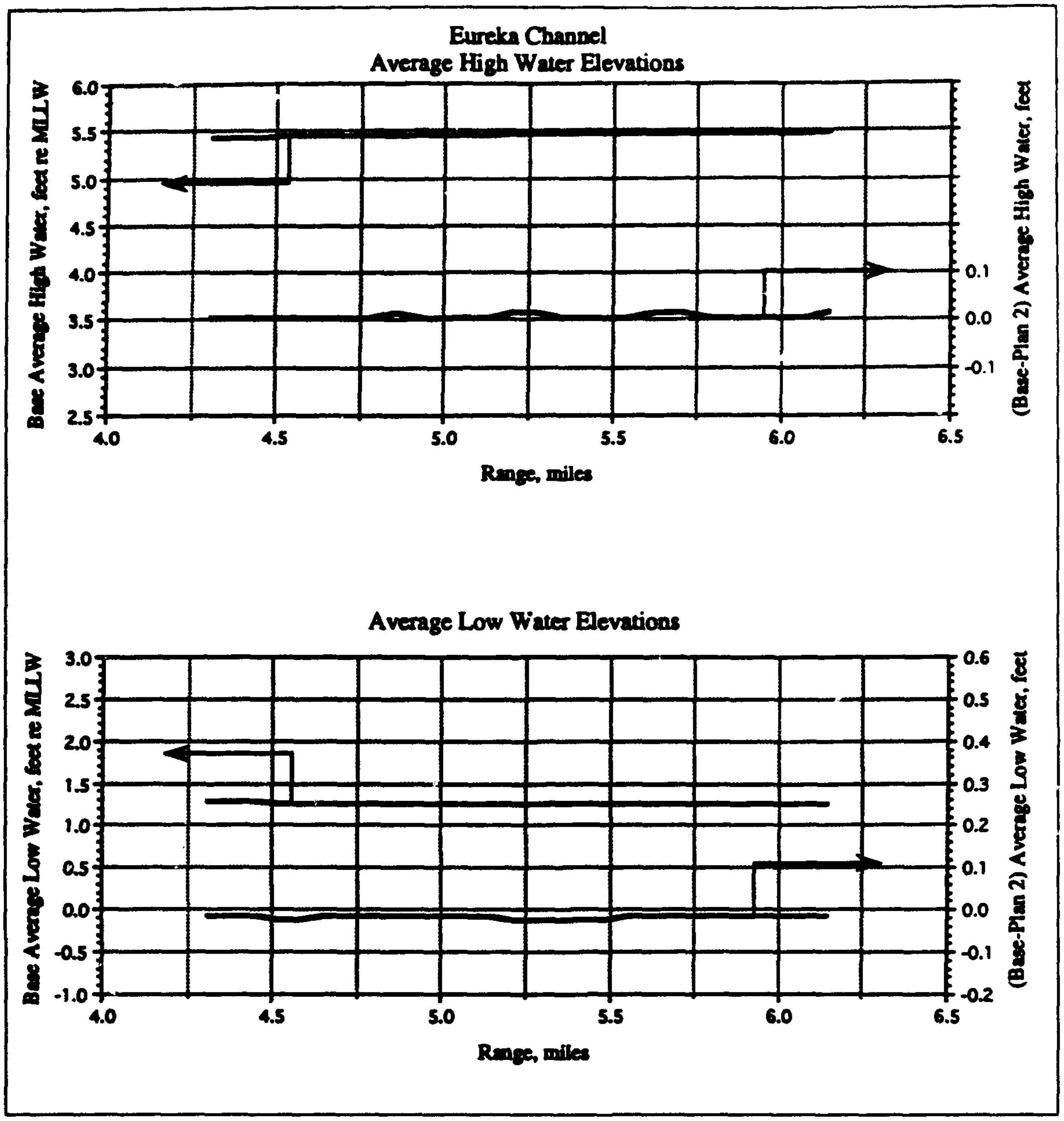

Figure 34. Average high and low water elevations, Base-Plan 2, Eureka Channel

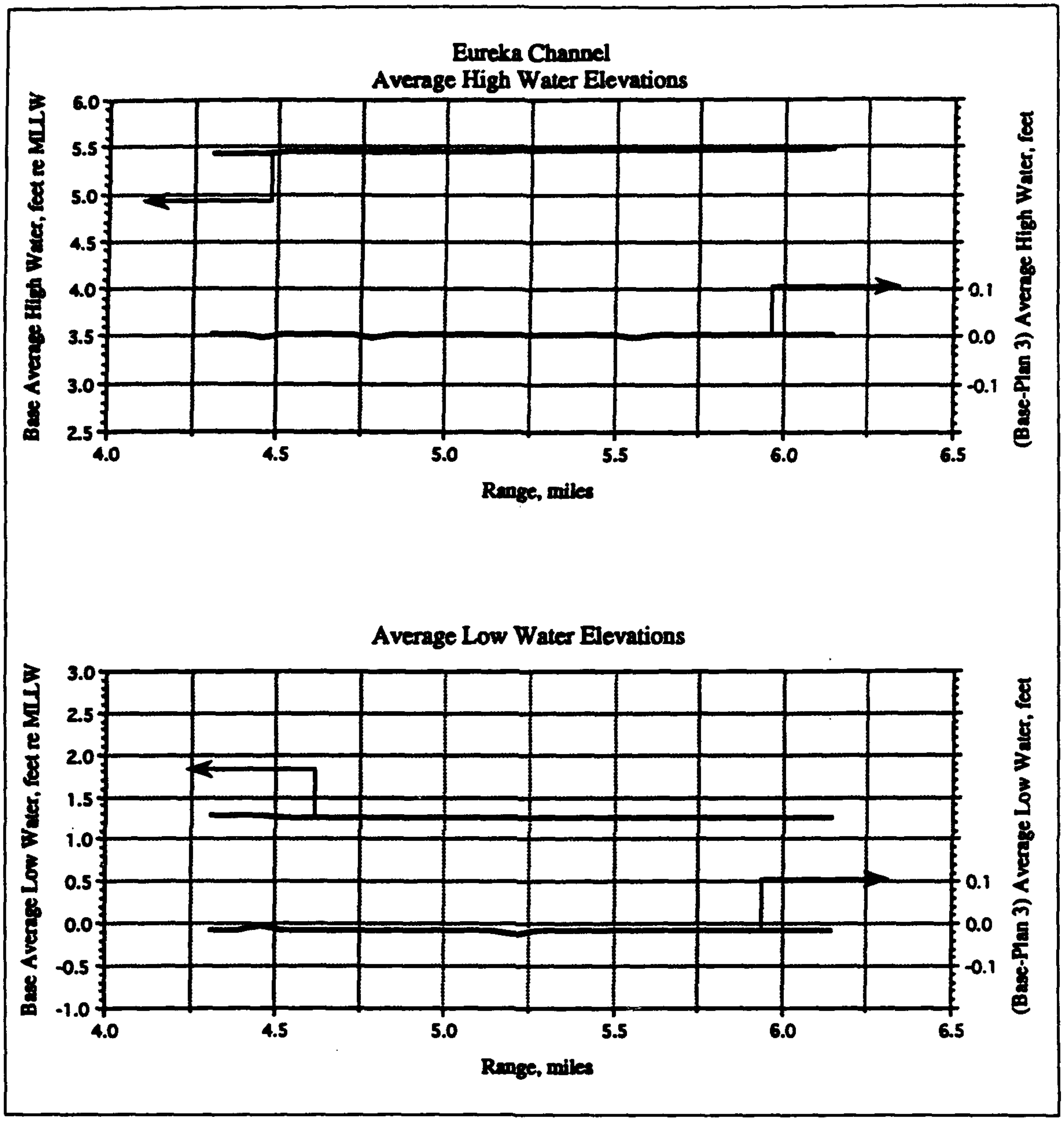

Figure 35. Average high and low water elevations, Base-Plan 3, Eureka Channel

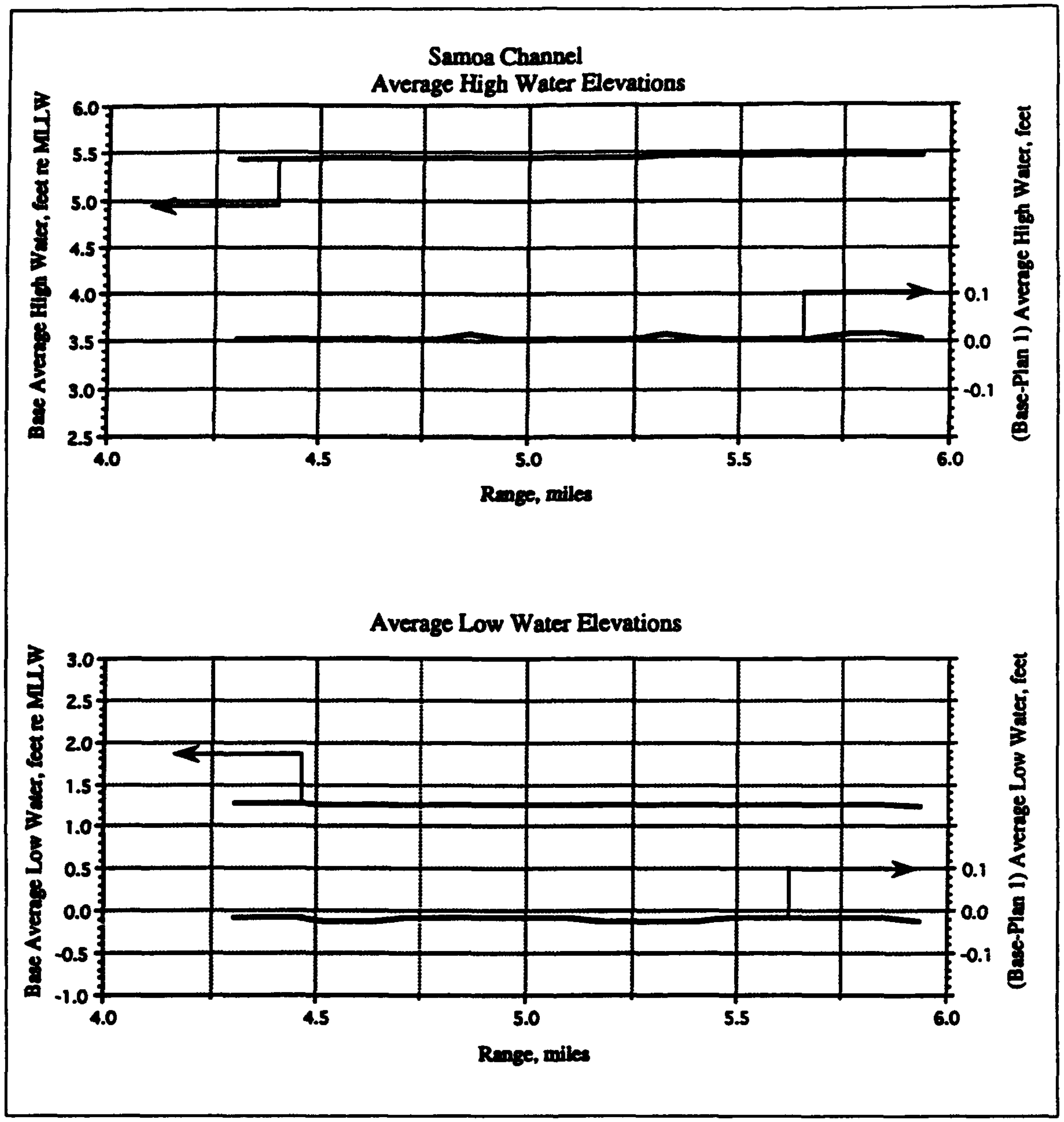

Figure 36. Average high and low water elevations, Base-Plan 1, Samoa Channel

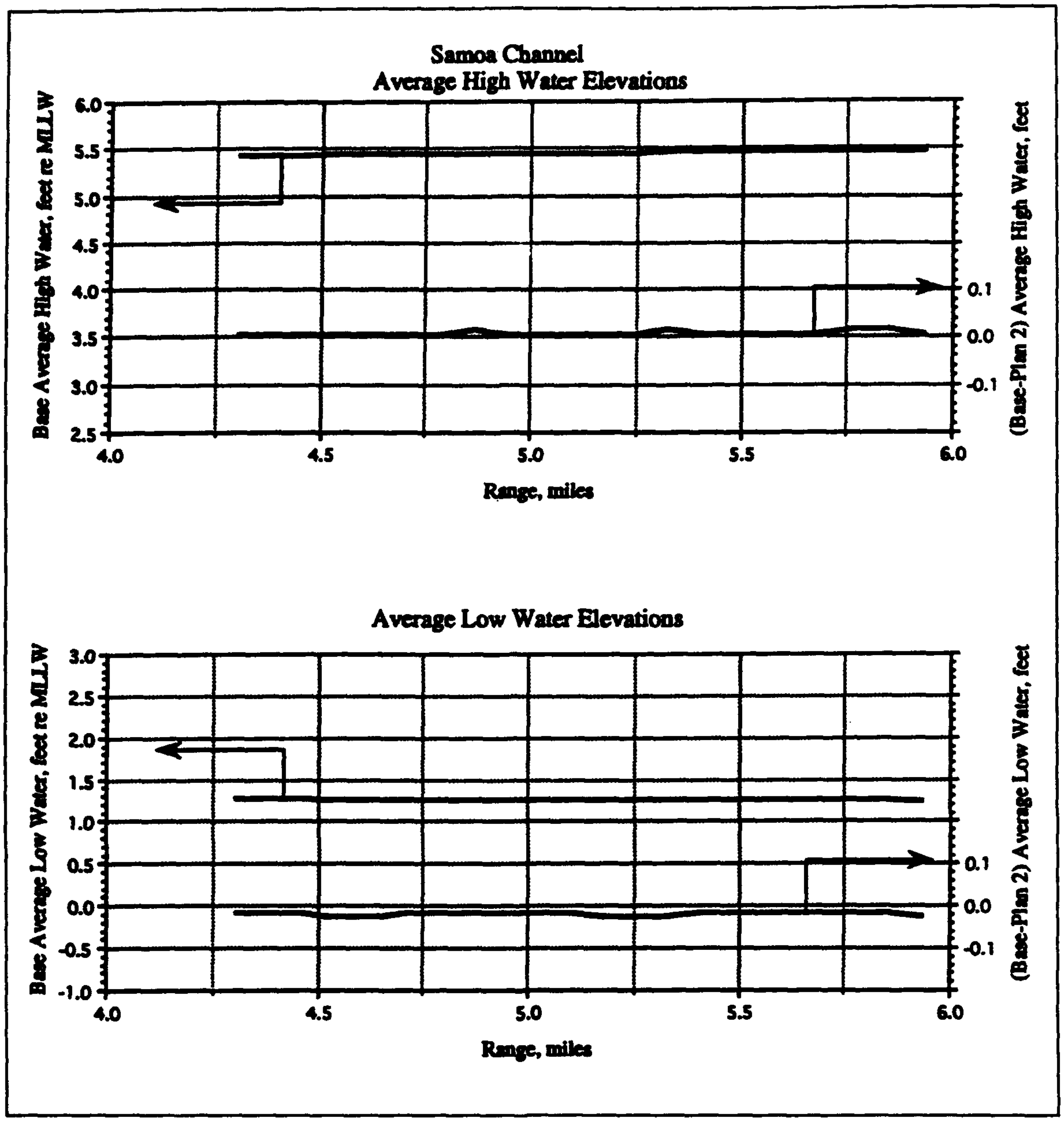

Figure 37. Average high and low water elevations, Base-Plan 2, Samoa Channel

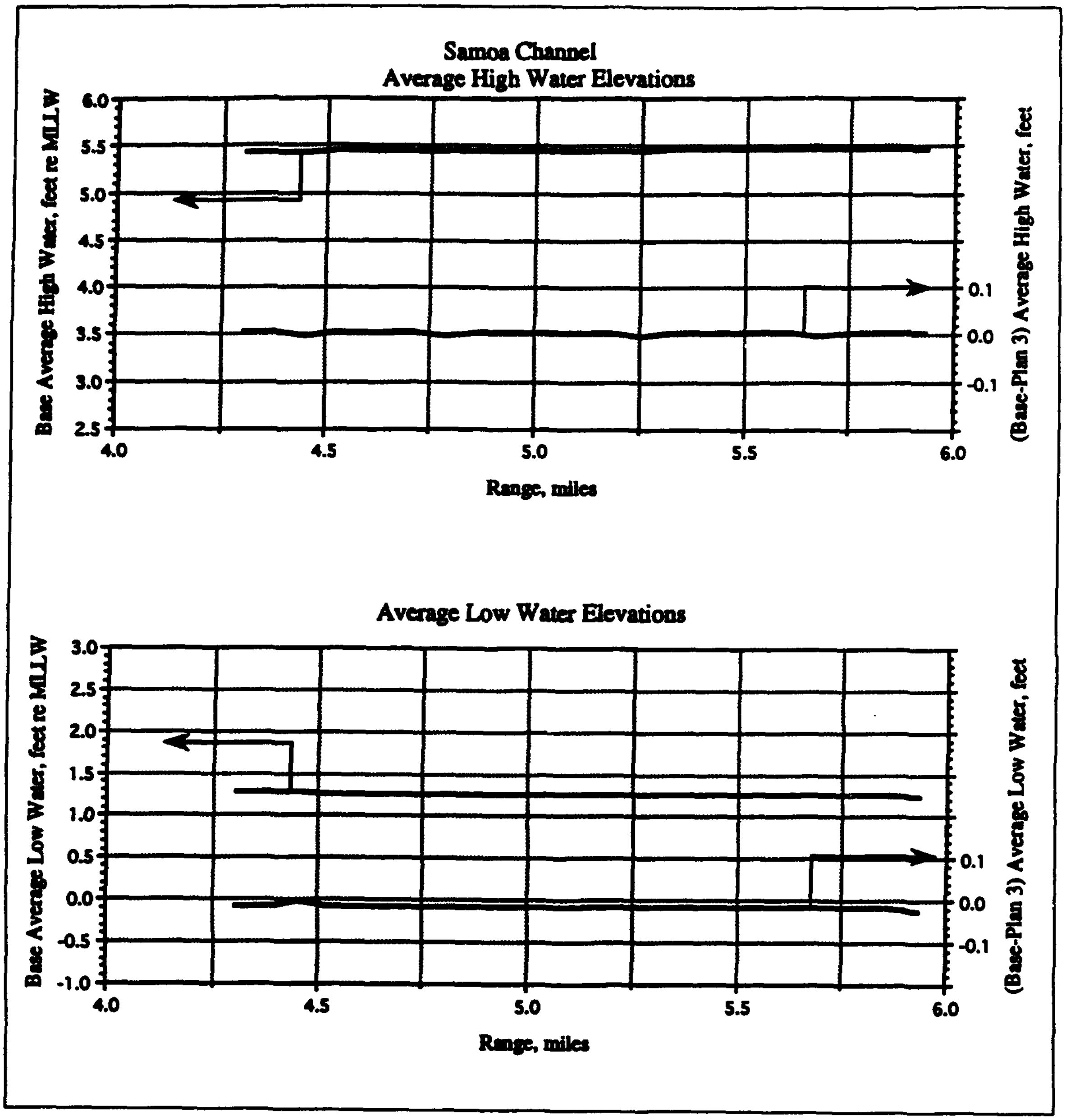

Figure 38. Average high and low water elevations, Base-Plan 3, Samoa Channel

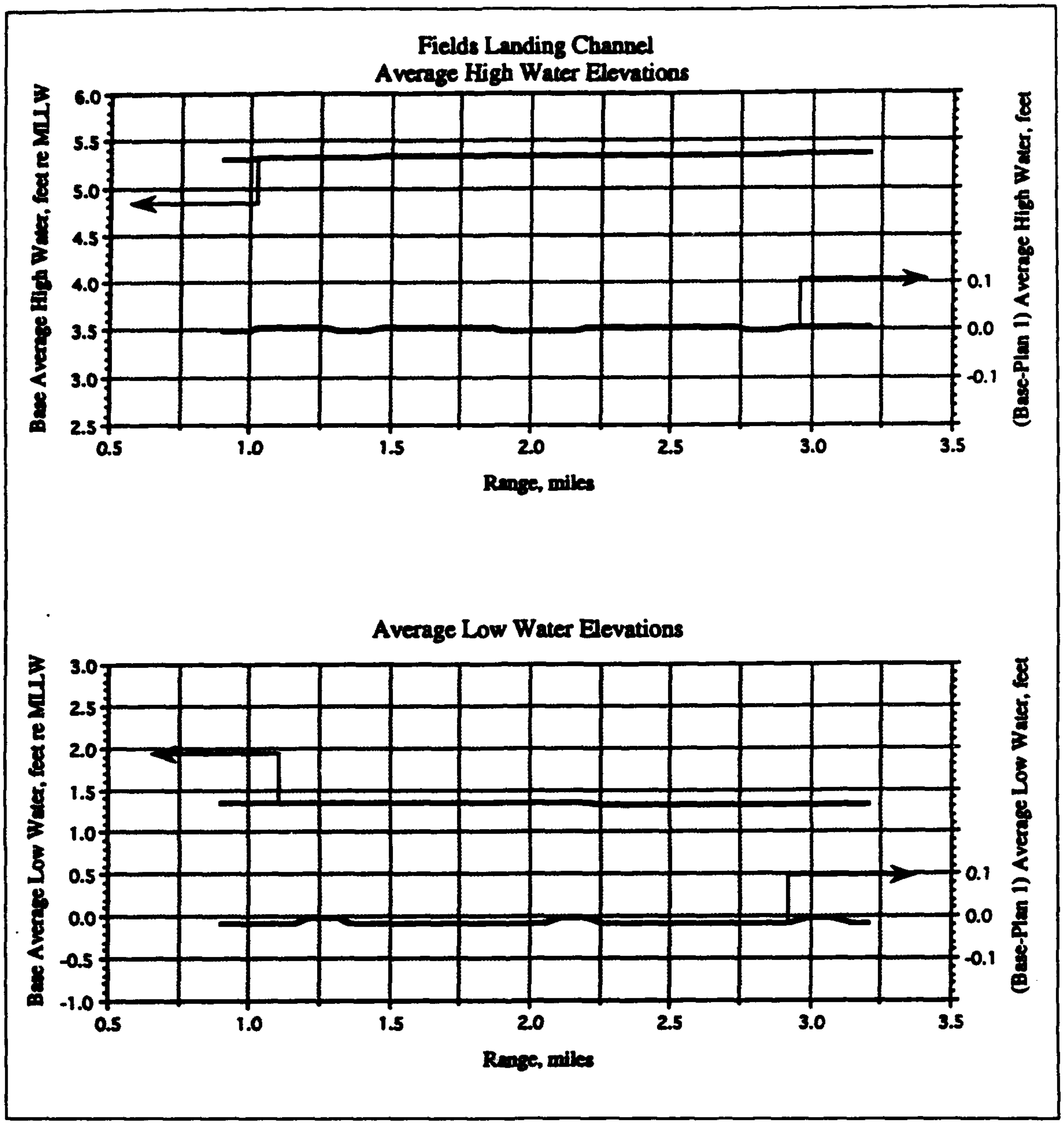

Figure 39. Average high and low water elevations, Base-Plan 1, Fields Landing Channel

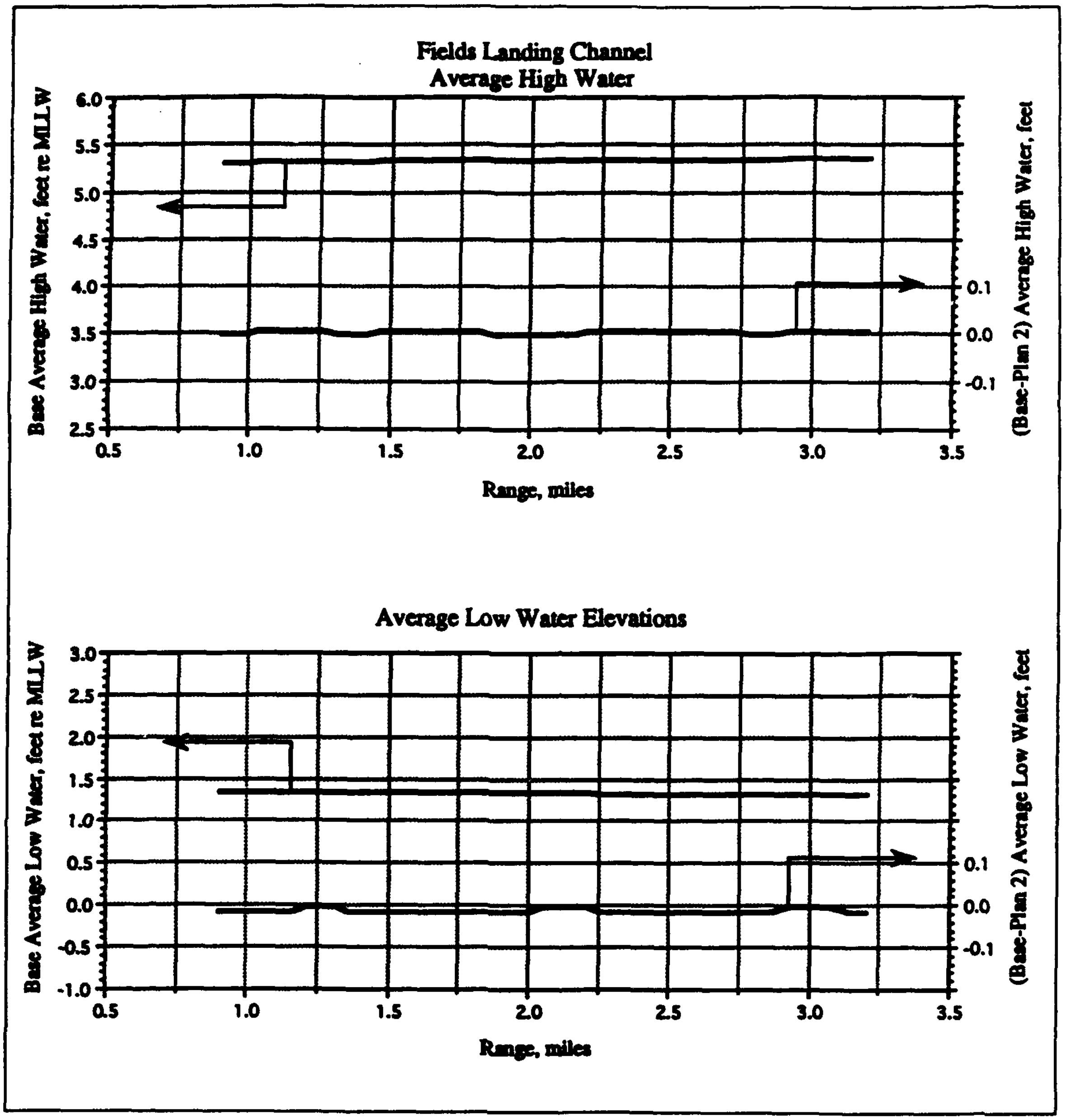

Figure 40. Average high and low water elevations, Base-Plan 2, Fields Landing Channel

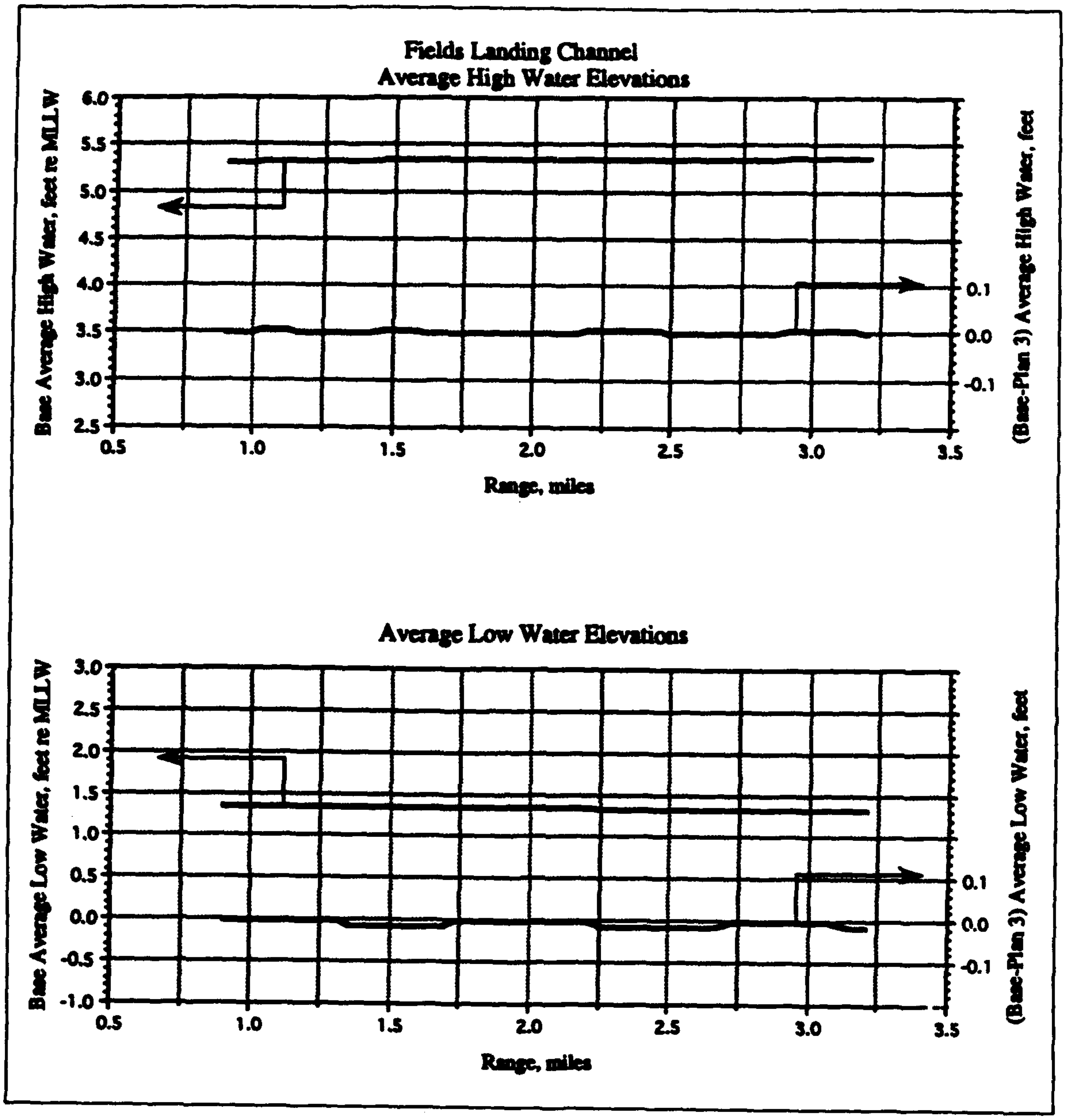

Figure 41. Average high and low water elevations, Base-Plan 3, Fields Landing Channel

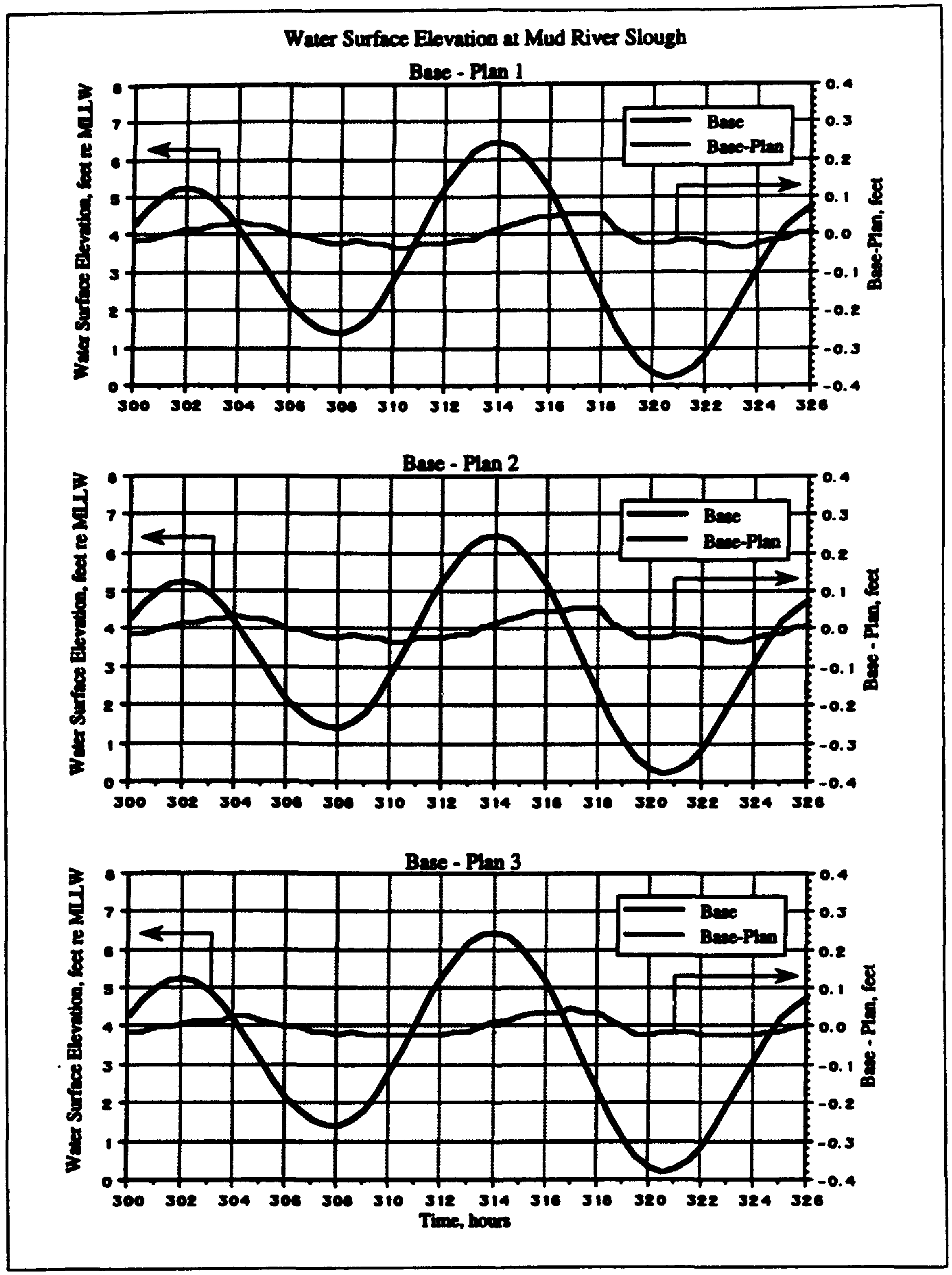

Figure 42. Mud River Slough water elevation differences

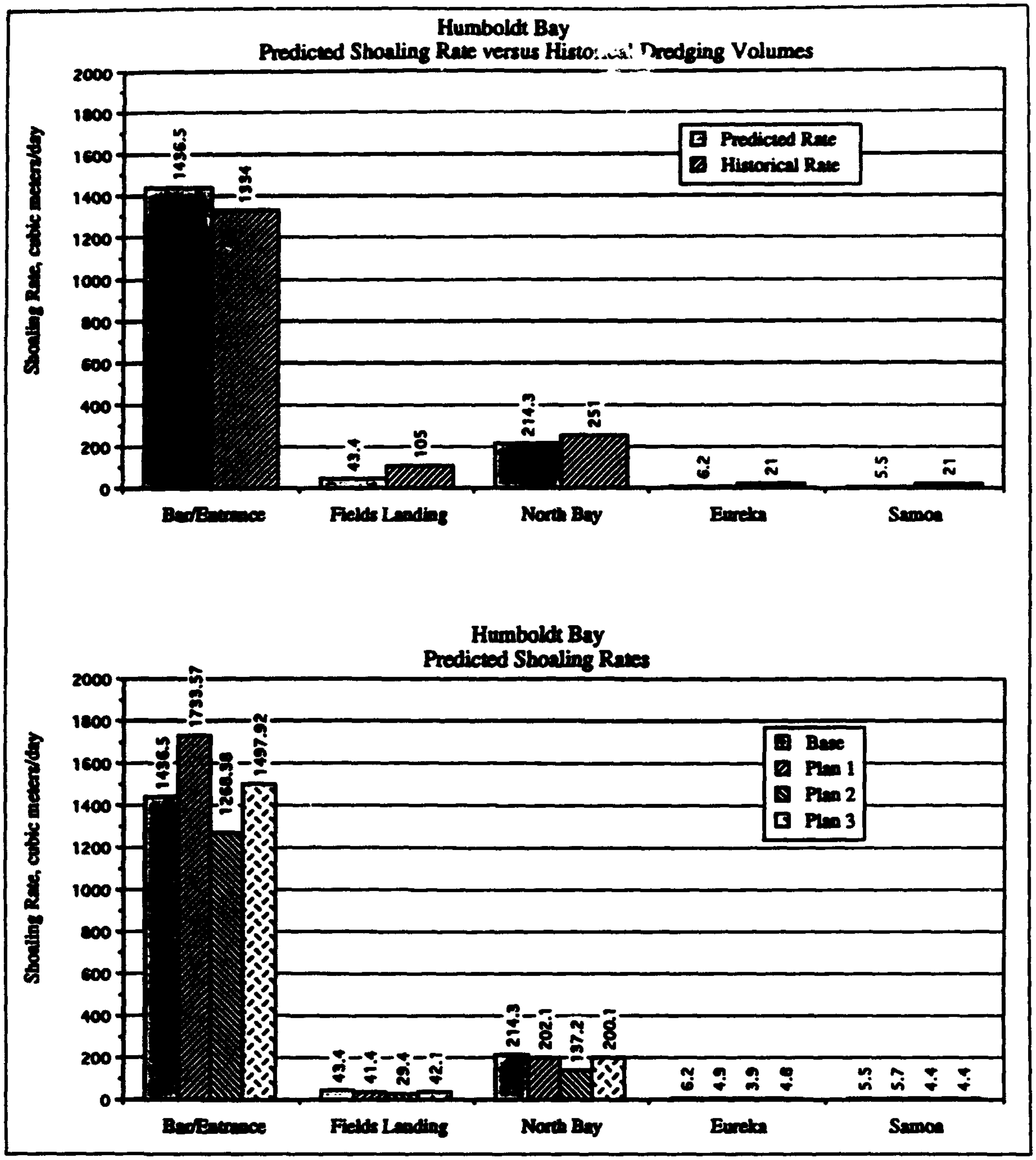

Figure 43. Humboldt Bay Channels sedimentation results

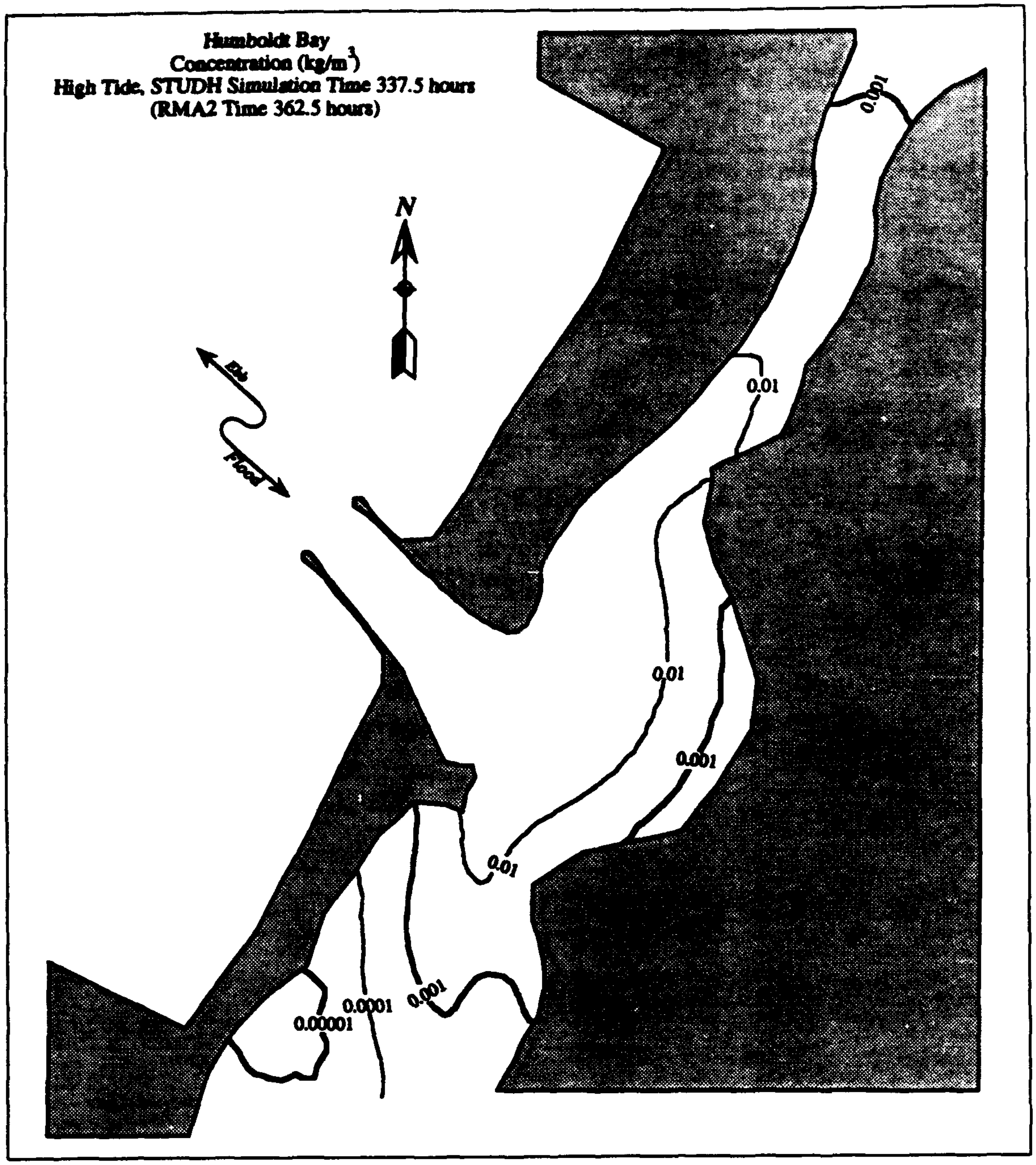

Figure 44. High tide sediment concentration contours

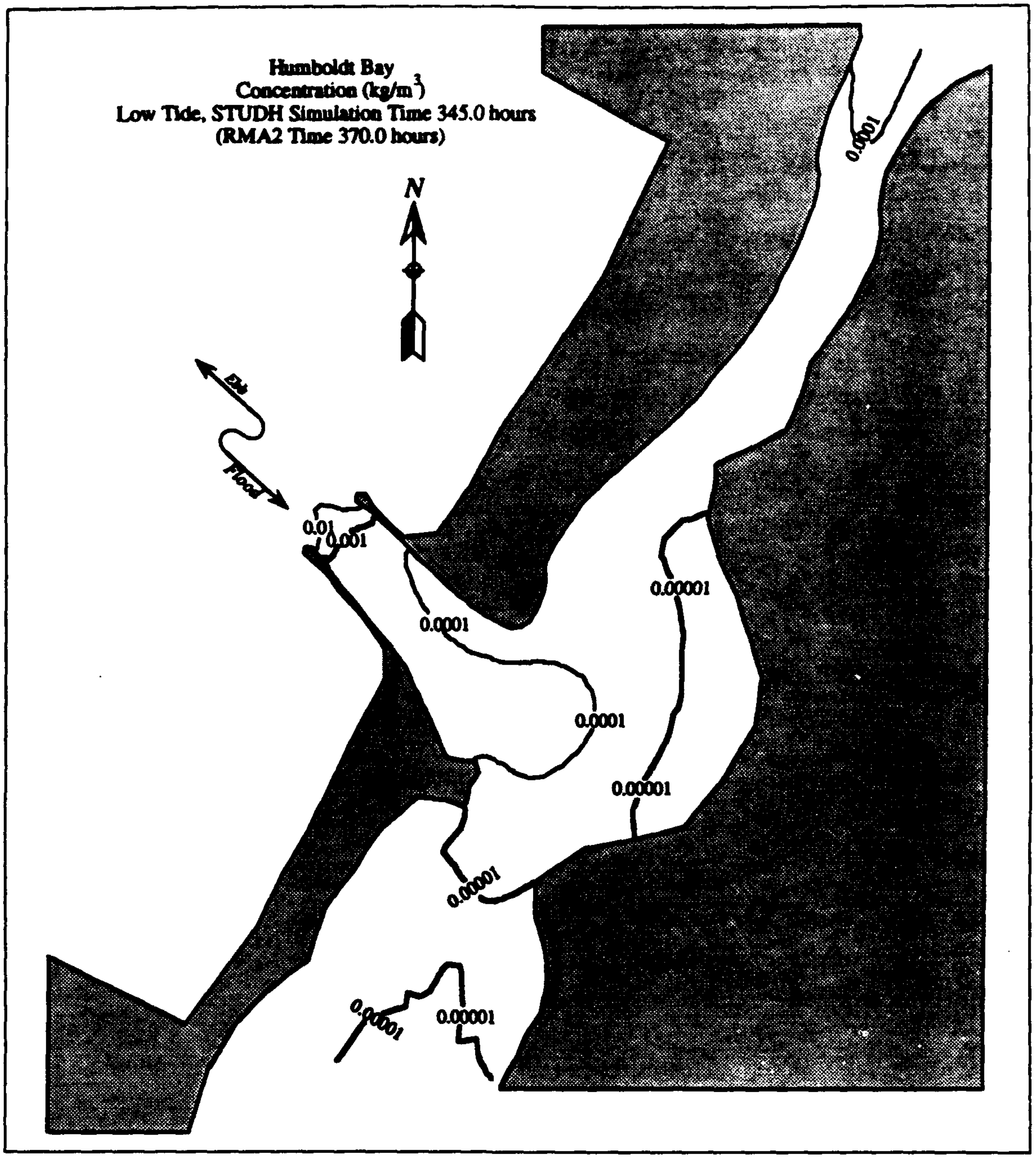

Figure 45. Low tide sediment concentration contours

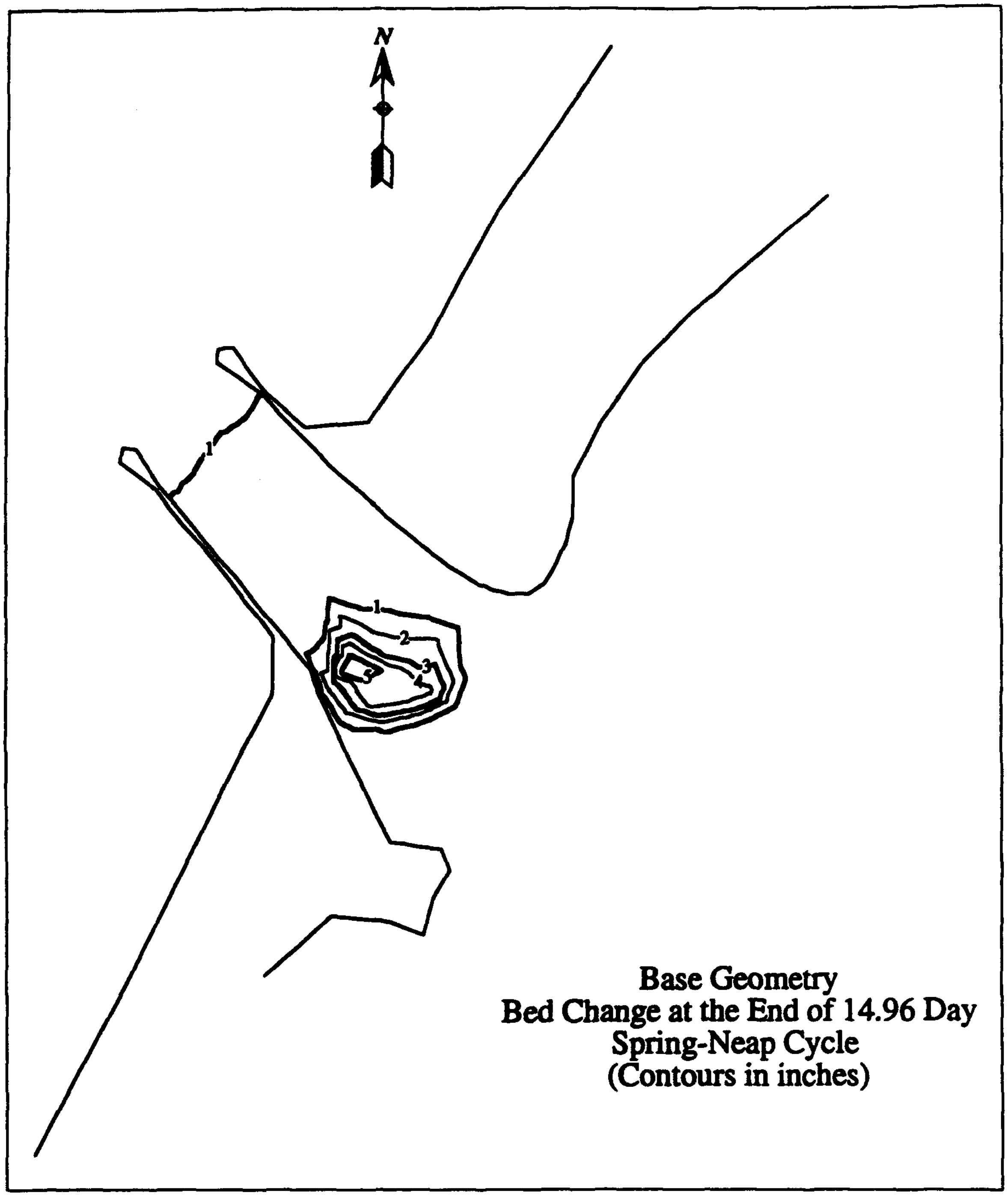

Figure 46. Bed change, Base

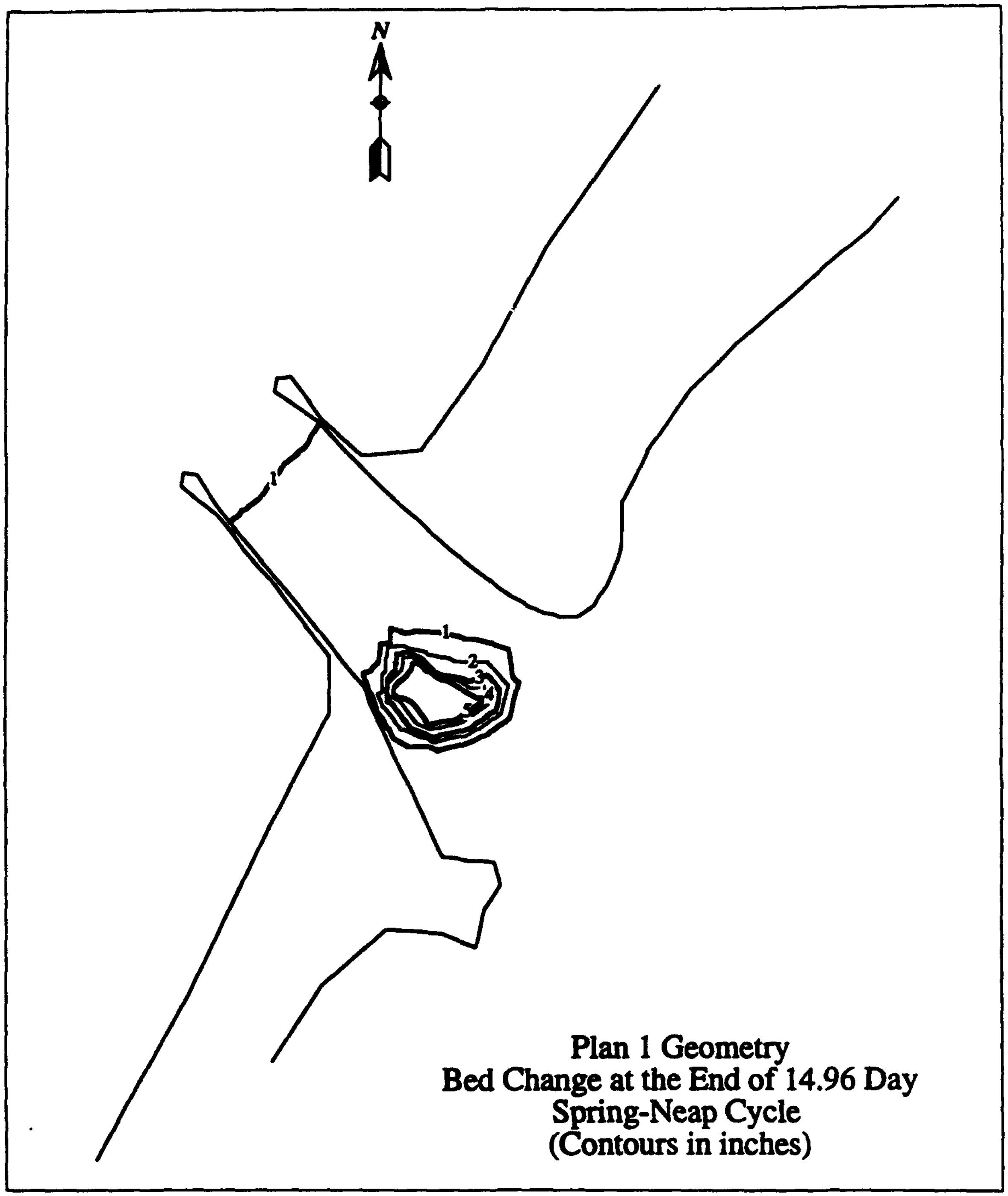

Figure 47. Bed change, Plan 1

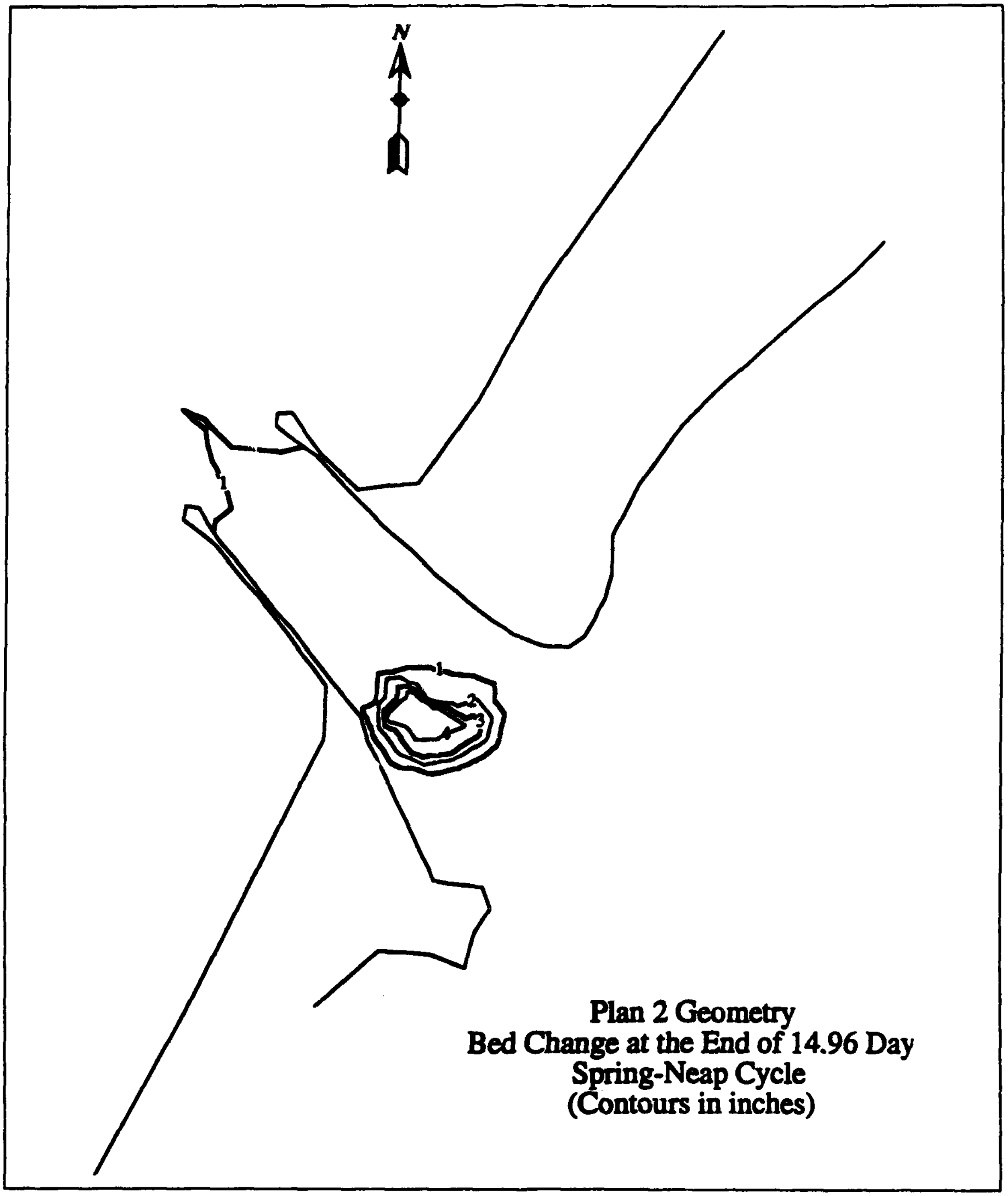

Figure 48. Bed change, Plan 2

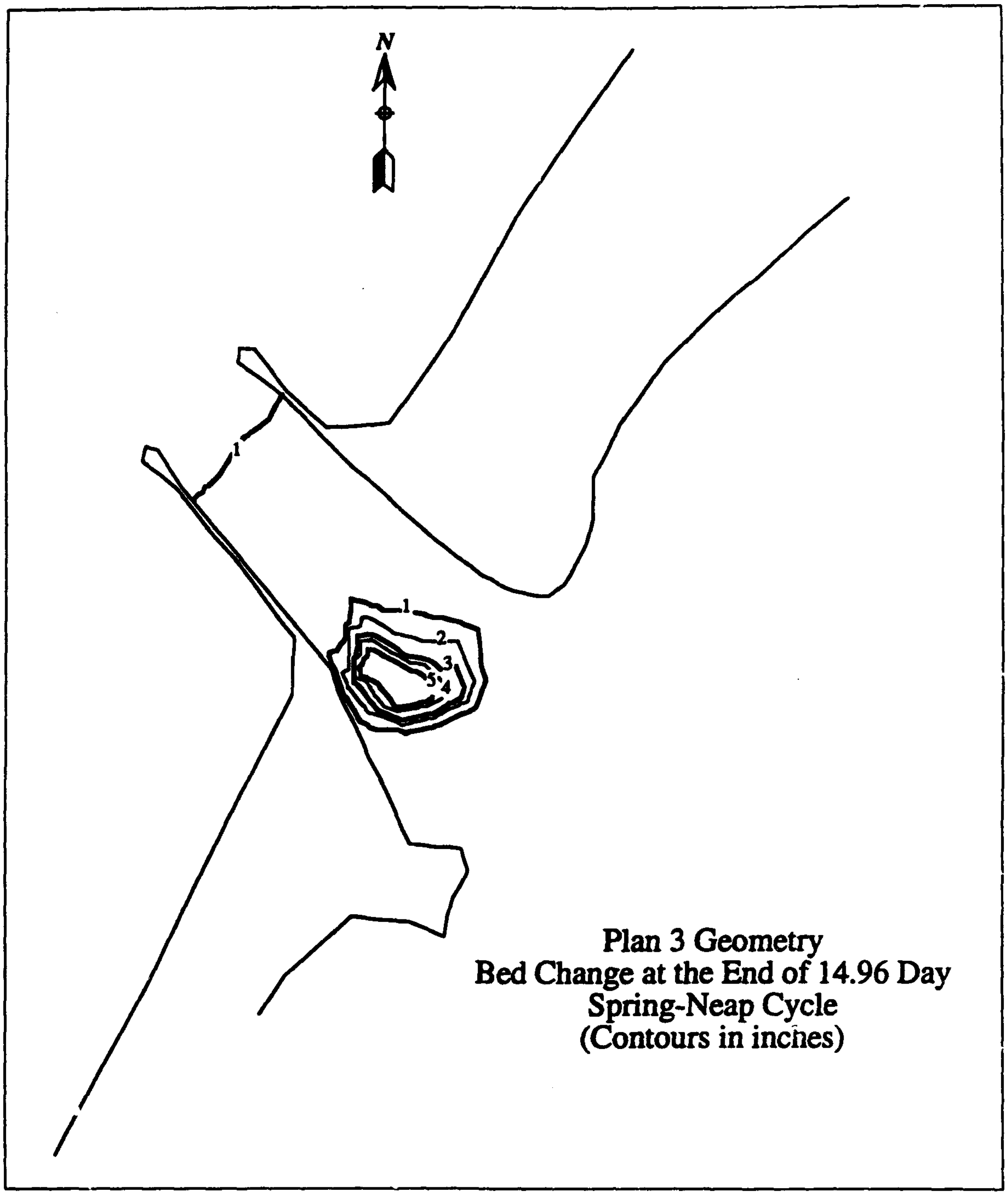

Figure 49. Bed change, Plan 3

REPORT DOCUMENTATION PAGE

Form Approved
OMB No. 0704-0188

1. AGENCY USE ONLY *(Leave blank)*

2. REPORT DATE
July 1994

3. REPORT TYPE AND DATES COVERED
Final report

4. TITLE AND SUBTITLE
Humboldt Bay Numerical Hydrodynamics and Sedimentation Study

5. FUNDING NUMBERS

6. AUTHOR(S)
Robert A. Evans, Jr.

7. PERFORMING ORGANIZATION NAME(S) AND ADDRESS(ES)
U.S. Army Engineer Waterways Experiment Station
3909 Halls Ferry Road
Vicksburg, MS 39180-6199

8. PERFORMING ORGANIZATION REPORT NUMBER
Miscellaneous Paper
HL-94-2

9. SPONSORING/MONITORING AGENCY NAME(S) AND ADDRESS(ES)
U.S. Army Engineer District, San Francisco
211 Main Street
San Francisco, CA 94105-1905

10. SPONSORING/MONITORING AGENCY REPORT NUMBER

11. SUPPLEMENTARY NOTES
Available from the National Technical Information Service, 5285 Port Royal Road, Springfield, VA 22161.

12a. DISTRIBUTION/AVAILABILITY STATEMENT
Approved for public release; distribution is unlimited.

12b. DISTRIBUTION CODE

13. ABSTRACT *(Maximum 200 words)*

A study was done on the hydrodynamics and sedimentation of Humboldt Bay, California. This was done to determine the effects of channel deepening and realignment on the currents and sedimentation patterns in the area. The hydrodynamics and sedimentation were modeled with the TABS-MD modeling system. The hydrodynamics were verified to National Ocean Survey (NOS) harmonic data, and the sedimentation patterns were verified by comparison with historical dredging records. Predictions of changes in currents and sedimentation patterns were made for three different plans.

14. SUBJECT TERMS
See reverse.

15. NUMBER OF PAGES
67

16. PRICE CODE

17. SECURITY CLASSIFICATION OF REPORT	18. SECURITY CLASSIFICATION OF THIS PAGE	19. SECURITY CLASSIFICATION OF ABSTRACT	20. LIMITATION OF ABSTRACT
UNCLASSIFIED	UNCLASSIFIED		

14. (Concluded).

Humboldt Bay
Numerical hydrodynamic modeling
Numerical sedimentation modeling
Sedimentation
TABS-MD numerical modeling system